ERRATUM PUBLISHED 10 APRIL 2025; SEE LAST PAGE



RESEARCH ARTICLE SUMMARY

MICROBIAL ECOLOGY

# A phage tail–like bacteriocin suppresses competitors in metapopulations of pathogenic bacteria

**Talia Backman, Sergio M. Latorre, Efthymia Symeonidi, Artur Muszyński, Ella Bleak, Lauren Eads, Paulina I. Martinez-Koury, Sarita Som, Aubrey Hawks, Andrew D. Gloss, David M. Belnap, Allison M. Manuel, Adam M. Deutschbauer, Joy Bergelson, Parastoo Azadi, Hernán A. Burbano*†, Talia L. Karasov*†**

**INTRODUCTION:** Understanding the factors influencing plant pathogen spread is vital for developing disease prevention strategies. Bacterial pathogens must overcome plant immunity, compete with microbes, and resist bacteriophages to colonize plants. Host genetics affect pathogen suppression, but the role of the surrounding microbiota remains unclear. Bacteriophage (phage), viruses of bacteria, and phage-derived elements are widespread entities that selectively kill bacteria. These elements, repurposed from phage ancestors, target co-occurring bacterial strains, potentially shaping microbial communities. Despite their prevalence, their impact on plant microbiota and pathogen spread remains largely unknown.

**RATIONALE:** Our previous work revealed that wild populations of *Arabidopsis thaliana*, unlike agricultural and clinical pathogen outbreaks, are colonized by genetically diverse *Pseudomonas* populations without dominant strains. Infections with *Pseudomonas viridiflava* comprised multiple co-occurring strains even within single plants. What prevents single pathogenic lineages from spreading? Host immune diversity likely contributes to pathogen diversity, but the plant microbiome may also play a role. Given the common occurrence of phage and phage-derived elements and their strain-specific killing activity in *Pseudomonas* populations, we hypothesized that differences in sensitivity to phage components could suppress specific strains.

**RESULTS:** We discovered an abundant viral cluster that is conserved across pathogenic strains. This cluster does not encode an intact phage but rather encodes a tailocin, a phage-derived element that bacteria use to kill bacterial competitors. Each pathogenic *Pseudomonas* strain carries one of a few distinct tailocin variants, which target variable polysaccharides in the outer membrane of co-occurring pathogens. Analysis of historic herbarium samples revealed that the same tailocin and outer membrane variants have persisted in the *Pseudomonas* populations for at least two centuries, suggesting the continued use of a defined set of tailocin haplotypes and receptors. Our results support a model in which the tailocin and outer membranes of co-occurring *Pseudomonas* strains are evolving in concert in wild *A. thaliana* populations. The divergent tailocin and outer membrane haplotypes have been maintained across time and space.

**CONCLUSION:** The presence of a limited set of tailocin haplotypes in the metapopulation could reflect a limited panel of resistance mechanisms. Our findings provide a roadmap for identifying tailocin specificities to different strains and the possibility of determining the mechanism of this specificity. Tailocin therapy, akin to phage therapy, holds promise as an alternative to traditional antibiotics. Initial studies demonstrate its efficacy in suppressing pathogens in various plant and animal models. However, as with any antimicrobial treatment, resistance may arise. Our results suggest that "tailocin cocktails" leveraging the genetic diversity of pathogens could mitigate resistance by targeting the metapopulation concurrently. ■

The list of author affiliations is available in the full article online.
*Corresponding author. Email: h.burbano@ucl.ac.uk (H.A.B.); t.karasov@utah.edu (T.L.K.)
†These authors contributed equally to this work.
Cite this article as T. Backman *et al.*, *Science* **384**, eado0713 (2024). DOI: 10.1126/science.ado0713

READ THE FULL ARTICLE AT
https://doi.org/10.1126/science.ado0713

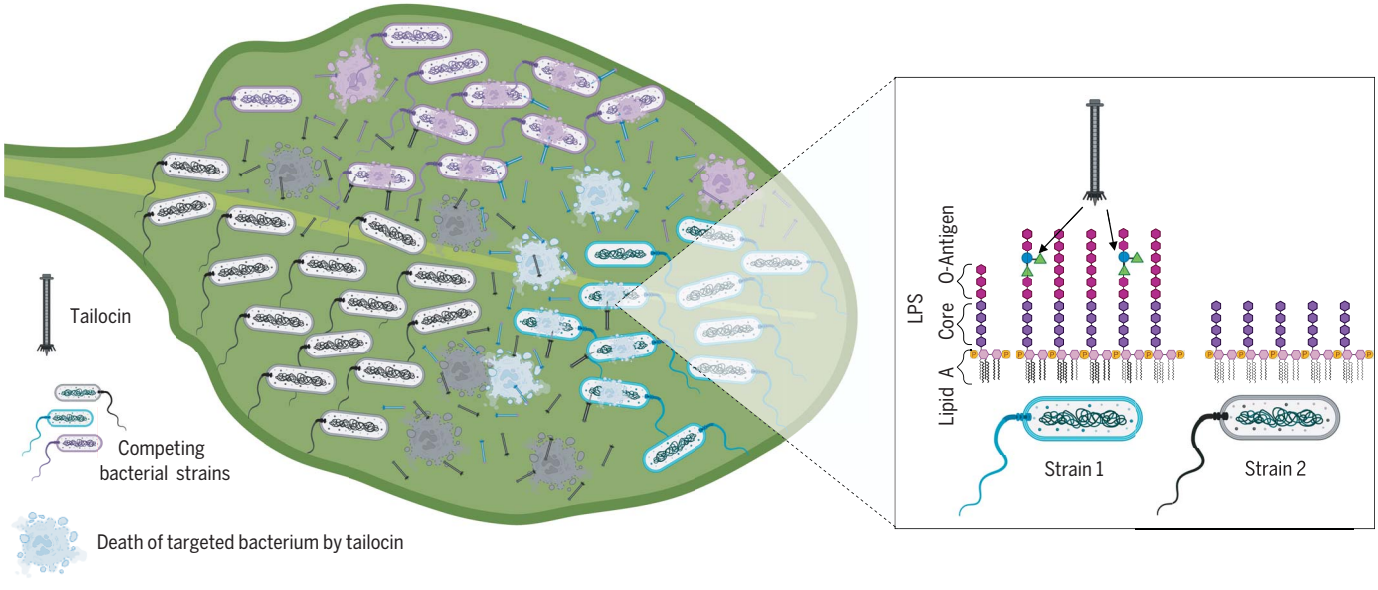


**Pathogenic bacterial competitors on a leaf surface deploy tailocins as antagonistic agents.** Tailocins are elements derived from bacterial viruses (bacteriophage) that have been repurposed to selectively target and kill strains of neighboring bacteria. The deployment of a diverse yet limited set of tailocins among pathogenic bacteria maintains their diversity over evolutionary timescales and shapes the coevolution of tailocins and their receptors in the outer membrane of targeted bacterial cells. [Figure created with BioRender.com]

ERRATUM PUBLISHED 10 APRIL 2025; SEE LAST PAGE



RESEARCH ARTICLE

MICROBIAL ECOLOGY

# A phage tail–like bacteriocin suppresses competitors in metapopulations of pathogenic bacteria

Talia Backman[1], Sergio M. Latorre[2,3], Efthymia Symeonidi[1], Artur Muszyński[4], Ella Bleak[1], Lauren Eads[1], Paulina I. Martinez-Koury[1], Sarita Som[1], Aubrey Hawks[1], Andrew D. Gloss[5], David M. Belnap[1,6], Allison M. Manuel[7], Adam M. Deutschbauer[8], Joy Bergelson[5], Parastoo Azadi[4], Hernán A. Burbano[2,3]*†, Talia L. Karasov[1]*†

**Bacteria can repurpose their own bacteriophage viruses (phage) to kill competing bacteria. Phage-derived elements are frequently strain specific in their killing activity, although there is limited evidence that this specificity drives bacterial population dynamics. Here, we identified intact phage and their derived elements in a metapopulation of wild plant–associated *Pseudomonas* genomes. We discovered that the most abundant viral cluster encodes a phage remnant resembling a phage tail called a tailocin, which bacteria have co-opted to kill bacterial competitors. Each pathogenic *Pseudomonas* strain carries one of a few distinct tailocin variants that target the variable polysaccharides in the outer membrane of co-occurring pathogenic *Pseudomonas* strains. Analysis of herbarium samples from the past 170 years revealed that the same tailocin and bacterial receptor variants have persisted in *Pseudomonas* populations. These results suggest that tailocin genetic diversity can be mined to develop targeted "tailocin cocktails" for microbial control.**

Understanding the factors that influence the spread of pathogens is fundamental for developing disease prevention and treatment strategies. To colonize a plant, bacterial pathogens not only need to overcome the plant's immune system, but they also must compete with surrounding microbes. Microbial disease is a frequent outcome in genetically homogeneous agricultural fields but rarer in genetically diverse wild plant populations (*1*). These wild plant populations are instead typically colonized at low levels by diverse pathogens, with no strain spreading widely (*2*). The prominent role of host genetics in suppressing pathogenic lineages is well documented (*3*), but how the surrounding microbiota affect disease dynamics remains largely unknown and is thus of increasing interest (*4*).

Bacteria have evolved diverse mechanisms of competition, and several of these mechanisms were repurposed from phage machinery (*5*, *6*). Repurposed phage elements include injection systems such as the type VI secretion system and phage tail–like bacteriocins (tailocins) (*6*) in which remnants of the phage injection system have been retargeted for competition between bacteria. A common feature of many phage-related injection systems is their specificity; they can target specific strains of a bacterial species while not affecting the remainder (*6*). These injection systems are also widespread across bacteria (*7*–*11*). Given their prevalence, repurposed phage remnants are hypothesized to be drivers of microbiome composition in host and nonhost environments (*6*). To date, the impact of phage-derived elements on plant microbiota has only been observed in the laboratory under controlled conditions (*12*, *13*). Whether these elements are a major suppressor of pathogen strains in the wild is a matter of speculation (*14*) [but see (*15*, *16*)].

We previously found that wild populations of the plant *Arabidopsis thaliana* were colonized by a genetically diverse metapopulation of *Pseudomonas* bacterial pathogens (*17*). Our prior results suggested that these pathogen populations do not undergo the clonal expansions observed in agricultural and clinical pathogens. Infections of *Pseudomonas viridiflava* populations, even within a single plant, consist of several co-occurring strains with no single strain becoming dominant (*2*). What prevents single pathogenic lineages from spreading? Immune diversity of the host plant *A. thaliana* plays a role in maintaining *Pseudomonas* pathogen diversity; however, our previous work indicated that other members of the plant microbiome also affect the *Pseudomonas* composition (*18*–*20*). Because phage and their derived elements are common in *Pseudomonas* populations (*21*) and can be strain specific in their killing activity (*22*), we hypothesized that differences in sensitivity to phage components and their derived elements could suppress specific *Pseudomonas* strains in our system.

## The viral cluster VC2 is strongly associated with a pathogenic clade of *P. viridiflava*

To determine whether phage-related elements are associated with turnover in the *Pseudomonas* colonizing *A. thaliana*, we first sought to characterize the abundant phage-homologous sequences in a wild *Pseudomonas* metapopulation. Viral sequences integrated within a bacterial genome can indicate a lysogeny event with a compatible phage (*23*). We characterized the presence and evolution of viral elements in 1524 *Pseudomonas* genomes all collected from *A. thaliana* in southwestern Germany (fig. S1) (*24*). More than 85% of these genomes are classified as the ATUE5 clade of *P. viridiflava* (Fig. 1A), an opportunistic pathogen that colonizes *A. thaliana* throughout Europe and the US (*25*, *26*). We found viral sequences in 99.3% of the genomes, with an average of two viral sequences per genome (Fig. 1B). By using pairwise k-mer distances (*27*) and subsequent k-means clustering, we identified four viral sequence clusters (Fig. 1C).

Phylogenetic associations between *Pseudomonas* clades and viral sequence clusters were immediately apparent (Fig. 1D) (*2*), with viral cluster 2 (VC2) found in all ATUE5 pathogenic strains, but they were less frequent (29%) (Fig. 1D) in nonpathogenic isolates outside of the ATUE5 clade. Furthermore, the gene composition and synteny of VC2 is conserved across ATUE5 strains but has divergent sequences outside the closest relatives to ATUE5 (Fig. 2B). The VC2 sequences in ATUE5 consist of 24 genes that are colinearly integrated in all genomes at the same location: between the *trpE* and *trpG* bacterial genes (*28*, *29*). These VC2 sequences are predicted to encode the structural components typical of a prophage, including base plates, tail spikes, tubes, sheaths, tail fibers, putative assembly chaperones, and transcriptional regulation proteins.

## VC2 encodes a structurally functional tailocin

Analysis of the VC2 gene content revealed that this cluster lacks the components necessary for phage replication and encapsulation, such as capsid, terminase, integrase, and recombinase proteins, suggesting that the VC2 genomic region does not encode a fully functional phage (*30*, *31*). Although the structure of VC2 was not consistent with a functional phage, it did resemble previously described phage tail–like bacteriocins derived from phage, which are referred to as tailocins (*32*). Tailocins are repurposed phages

[1]School of Biological Sciences, University of Utah, Salt Lake City, UT 84112, USA. [2]Centre for Life's Origins and Evolution, Department of Genetics, Evolution and Environment, University College London, London WC1E 6BT, UK. [3]Research Group for Ancient Genomics and Evolution, Department of Molecular Biology, Max Planck Institute for Biology, 72076 Tübingen, Germany. [4]Complex Carbohydrate Research Center, University of Georgia, Athens, GA 30602, USA. [5]Center for Genomics and Systems Biology, New York University, New York, NY 10003, USA. [6]Department of Biochemistry, University of Utah, Salt Lake City, UT 84112, USA. [7]Mass Spectrometry and Proteomics Core, The University of Utah, Salt Lake City, UT 84112, USA. [8]Environmental Genomics and Systems Biology Division, Lawrence Berkeley National Laboratory, Berkeley, CA 94720, USA.
***Corresponding author. Email: h.burbano@ucl.ac.uk (H.A.B.); t.karasov@utah.edu (T.L.K.)**
†These authors contributed equally to this work.

ERRATUM PUBLISHED 10 APRIL 2025; SEE LAST PAGE



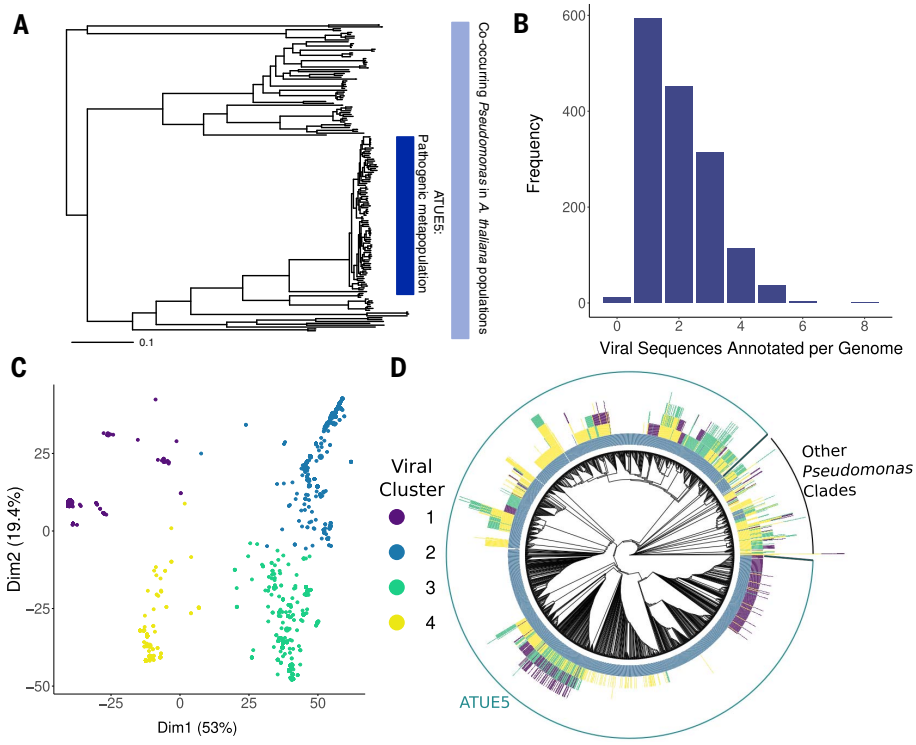


**Fig. 1. The pathogenic clade of *P. viridiflava* ATUE5 harbors a single highly conserved viral cluster (VC2).** (**A**) Maximum likelihood concatenated core genome phylogeny of 1524 pseudomonads that co-occur in the *A. thaliana* phyllosphere (light blue bar). The dark blue bar indicates a pathogenic clade of *P. viridiflava* ATUE5 [adapted from Karasov *et al*. (*2*)]. (**B**) Frequency of viral elements identified in each *Pseudomonas* genome. Each genome harbors between one and eight viral elements. (**C**) Principal component analysis of viral elements based on pairwise k-mer Mash distances (*27*) and silhouette analysis reveals four defined clusters. Points are colored as indicated in the inset. (**D**) Viral elements of VC2 are present in all genomes of the pathogenic operational taxonomic unit (OTU) ATUE5. The phylogeny shows the relationships among 1524 *Pseudomonas* strains. Each stacked bar around the phylogeny indicates the presence of a viral element (with a maximum height of eight viral elements). The bars are colored as in (C). The outer circle shows strains that belong to ATUE5 (green) and other OTUs (black).

that bacteria use to kill co-occurring bacterial strains (*28*) using the targeting machinery of the phage ancestor (*33*).

To test whether the tailocin genomic island produces the predicted tailocin protein complex, we induced tailocin production in a representative strain of ATUE5 (p25.A12) using treatment with mitomycin C (MMC) (*34*), partially purified the lysate, and then performed transmission electron microscopy (TEM). TEM images (Fig. 2C and fig. S2) revealed one rod-like tailocin in the MMC-induced lysates of p25.A12 existing in both the extended (sheath-uncontracted) and contracted (sheath-contracted and tube-ejected) forms (Fig. 2C). The rod-like structures suggest that this tailocin is an R-type contractile tailocin (*35*–*37*). Image comparison of the two tailocin forms indicated that the tailocins differ in average length: The contracted tailocins were on average 130 nm, whereas the extended tailocins were on average 144 nm in length. No other intact phage or bacteriocin-like structures were observed in the TEM images, only apparent sheath assemblies without tubes (fig. S2).

To validate that the observed tailocin in the TEM image corresponded to our predicted tailocin from VC2, we performed untargeted data dependent liquid chromatography–tandem mass spectrometry (LC-MS/MS) proteomics analysis (*28*, *38*). Proteomics data confirmed the presence of tailocin proteins annotated in VC2 (Fig. 2B and table S1). No tailocin proteins were found in the sample that was not induced with MMC, and no other viral proteins or proteinaceous toxins such as S-bacteriocins were detected in the tailocin lysates. These results suggest that the highly conserved ATUE5 viral sequence is an active and inducible R-type tailocin.

### Co-occurring *Pseudomonas* genomes encode highly diverse tailocin variants

The phylogenetic distribution of the VC2 cluster (Figs. 1 and 2B) suggested that the VC2 genomic island is well conserved across pathogenic ATUE5 strains. Across the 1524 *Pseudomonas* genomes analyzed (Fig. 2D), the full complement of the 27 tailocin genes was found in >95% of ATUE5 genomes, suggesting that the tailocin is in the core genome of ATUE5 strains along with essential bacterial genes (*39*). The conservation of the tailocin protein complex across all ATUE5 genomes, its conserved content, and its consistent location between *trpE*/*trpG* (*32*) suggests a single integration of the VC2 tailocin in the common ancestor of ATUE5 that is likely important for fitness in its natural ecological context.

In addition to the conservation of its gene content and collinearity, we found that the VC2 cluster harbors average levels of intralineage nucleotide diversity comparable with bona fide *Pseudomonas* core genes (Fig. 2A and fig. S3A), indicating that the VC2 cluster has likely been evolving under similar levels of selective constraint. However, by calculating nucleotide diversity for each of the VC2 genes individually, we identified greater levels of nucleotide diversity in two tailocin genes, the *hypothetical tail fiber* (*HTF*) and the *tail fiber assembly* (*TFA*) genes. Moreover, these two genes were also outliers for positive values of Tajima's D (Fig. 2A and fig. S3B), a measure of the skewness of the site frequency spectrum (SFS), which in this case might indicate gene genealogies with deep divergence times and the likely existence of distinct haplotypes. It has been previously shown that the *HTF* and *TFA* genes together are key determinants of bacterial host range (*40*), which could explain their high level of diversity and the likely presence of multiple haplotypes.

We formally ascertained 40 and 25 haplotypes for *HTF* and *TFA*, respectively. In both cases, the five most common haplotypes accounted for ~80% of the *Pseudomonas* strains. The *HTF* haplotypes exhibited polymorphism in terms of their sequence length, with most falling into four distinct length categories (Fig. 3A). The *HTF* and *TFA* haplotypes are significantly associated (fig. S4, Fisher's exact test, $P = 0.0005$). The high positive values of Tajimas's D suggest that the divergent *HTF* and *TFA* haplotypes might have been maintained in the ATUE5 clade for long evolutionary times. Our population genomic analyses suggested that although the presence of the tailocin is conserved in pathogenic ATUE5 populations, the different ATUE5 strains encode one of a few divergent tailocin variants, with possible differences in binding and killing activity between the variants.

### Different tailocin variants kill closely related pathogenic *Pseudomonas*

We hypothesized that like other tailocins, the tailocin variants encoded by the *Pseudomonas* strains are used for interference competition against closely related competitor strains (*28*, *41*). Our system provides an opportunity

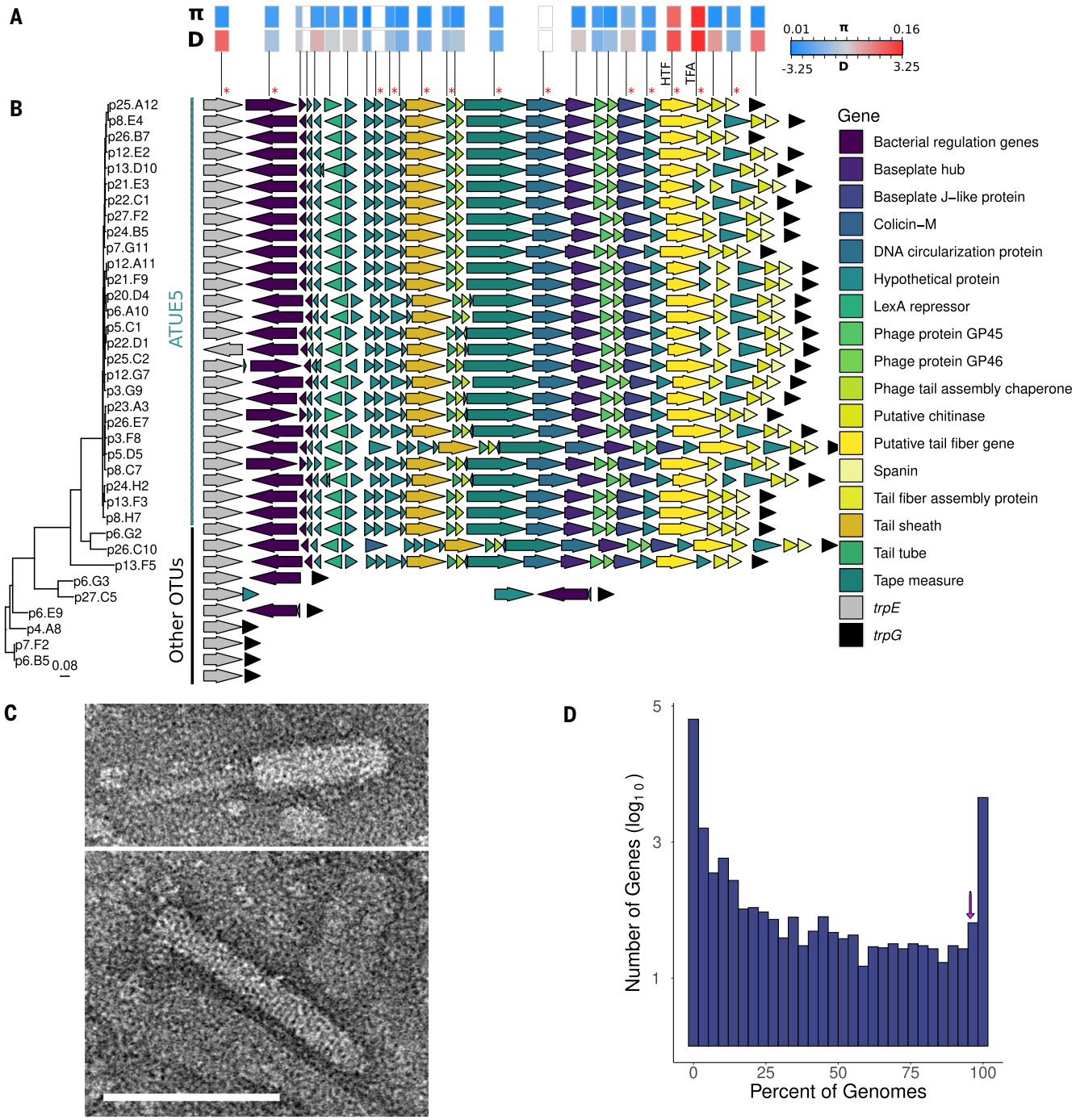


**Fig. 2. VC2 encodes a structurally functional tailocin.** (**A**) Within-lineage measures of nucleotide diversity measured as pairwise nucleotide differences ($\pi$) and the site frequency spectrum measured as Tajima's D (D) for each tailocin gene. White boxes indicate genes (statistics are excluded). Red asterisks indicate proteins found in proteomics analysis. (**B**) Genes of VC2 viral elements are syntenic in genomes of ATUE5. The arrows represent tailocin genes and surrounding bacterial genes (gene names are color coded in the inset). Each row is organized according to its phylogenetic placement. The phylogeny includes 36 *Pseudomonas* representative strains. The vertical lines indicate strains that belong to ATUE5 (green) and other OTUs (black). (**C**) TEM image demonstrates the presence of an assembled tailocin, showing the induced and partially purified tailocin from one representative ATUE5 strain (p25.A12) in both its contracted (top) and (bottom) uncontracted forms. Scale bar indicates 100 nm and applies to both micrographs. (**D**) The tailocin is part of the ATUE5 core genome. The histogram shows the frequency of each of the pangenome genes within 1399 ATUE5 genomes. The 11 most conserved tailocins genes are present in >90% of the ATUE5 genomes (marked with a purple arrow in the histogram).

ERRATUM PUBLISHED 10 APRIL 2025; SEE LAST PAGE



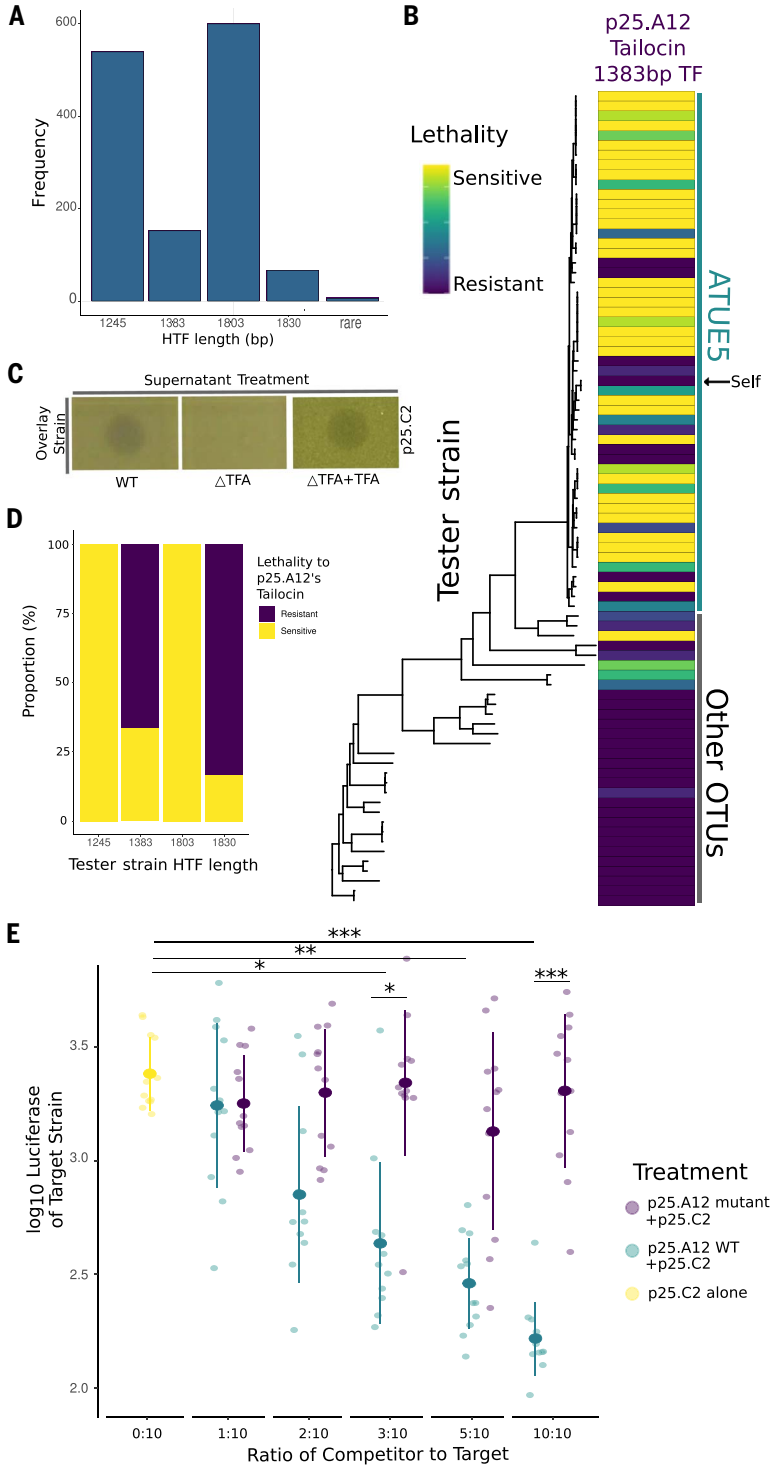


**Fig. 3. Tailocins target closely related pathogens.** (**A**) Frequency of HTF nucleotide sequence lengths. There are four highly conserved lengths within the *Pseudomonas* populations. (**B**) Tailocins are preferentially used for intralineage killing. Soft agar cultures of the *Pseudomonas* strains (rows) were challenged with viral particles extracted from cultures of one strain, p25.A12 (from the 1383-bp hypothetical tail fiber length haplotype, column), in three technical and three biological replicates. The phylogeny includes 83 *Pseudomonas* representative strains and is displayed according to phylogenetic placement. Vertical lines indicate strains that belong to ATUE5 (green) and other OTUs (gray). Interactions with the strain's own tailocin are indicated by the black arrow pointing to self. For each replicate, a strain was given a score of 3 for clear zone of inhibition, a 2 for semiclear, a 1 for opaque, or a 0 for no killing, and then added together after all three replicates. (**C**) Knockout of the tail fiber assembly gene disrupts tailocin bactericidal activity. Killing activity is indicated by a clearing in the lawn of the overlay strain. Complementation of the gene on an overexpression plasmid in the knockout strain restores the killing phenotype. (**D**) The proportion of tester strains sensitive or resistant to p25.A12's tailocin, a 1383-bp hypothetical tail fiber, significantly correlated with the tester strain's hypothetical tail fiber length haplotype (Fisher's exact test, $P = 10^{-8}$). (**E**) In planta coinfections of p25.A12 (competitor) and p25.C2 (target, known to be sensitive to p25.A12). Different ratios of competitor and constant amounts of target strain were used. p25.C2 was grown alone as the control. ANOVA test *P* values are shown. ***$P < 0.001$, **$P < 0.01$, or *$P < 0.05$.

to characterize the killing activity of tailocins produced by co-occurring microbes in the same wild plant populations. The relatedness of these microbes spans the spectrum from closely related (ATUE5, <1% genome-wide sequence divergence) to distant commensals (other ATUEs, >20% genome-wide sequence divergence).

We hypothesized that the ATUE5 tailocin is used for interference competition against (i) other pathogenic pseudomonads that also produce a tailocin, (ii) commensal pseudomonads that mostly do not produce the VC2 tailocin, or (iii) other bacterial strains in the phyllosphere community. To test this, the tailocins from three strains and two representative HTF length haplotypes were induced and then partially purified, and then concentrated tailocin lysates were applied to 55 ATUE5 strains, 28 other ATUE strains, and >50 other bacterial strains isolated from the phyllosphere (taxonomy unknown). We found that, as expected, ATUE5 strains were resistant to their own produced tailocin (*28*). The killing assay also revealed that non-ATUE5 *Pseudomonas* strains were sensitive in only 6% of ATUE5-derived tailocin treatments, whereas 40% of ATUE5 treatments with ATUE5-derived tailocins exhibited sensitivity (Fig. 3B and fig. S6). To

test whether other non-*Pseudomonas* community members were sensitive to the tailocin treatments, we tested 50 colonies (taxonomy and diversity unknown) from the surrounding phyllosphere and found that none was sensitive to tailocin treatment. An agriculturally relevant *Pseudomonas* strain, DC3000, was also tested and found to be sensitive to one of the tested tailocins (p25.A12). The different tailocin variants appear to exhibit partial killing specificity to different subsets of other ATUE5 pathogenic *Pseudomonas*, only 6% of the other *Pseudomonas* commensals, and not to other phyllosphere strains except for the above-mentioned DC3000.

To verify that the tailocin was responsible for the observed killing activity, we generated a TFA-deficient mutant. Tailocins collected from the mutant (p25.A12ΔTFA) lost killing activity against all strains tested (Fig. 3C and fig. S5), and the killing phenotype could be restored with an overexpression plasmid containing the *TFA* gene. These results suggest that tailocin was necessary for the observed killing activity.

To determine whether the TFA or HTF haplotypes are associated with killing activity, we analyzed whether the tailocin-killing spectrum correlates with a bacterial tester strain's TFA or HTF haplotype. Rather than a correlation, we found an array of different killing spectra, with the tail TFA and/or HTF haplotypes tested all displaying broad killing against other ATUE5 strains (Fig. 3B and fig. S6). Although we found there to be no significant associations between killing spectra and TFA or HTF haplotype, we did identify a significant association between the length of the HTF and its killing spectrum (Fig. 3, A and D, Fisher's exact test, $P = 10^{-8}$). This suggests that the tail fibers in the characterized tail fiber sequence length haplotypes could be important in binding to target cells, and that the tail fiber haplotypes are likely associated with an outer membrane receptor gene.

We next aimed to determine whether tailocin killing is observed in the plant host. We performed competition assays in planta. Strain p25.12's tailocin was able to kill a particularly pathogenic strain, p25.C2, in all three killing assays (Fig. 3B, third row). To test whether the target strains would also be killed by the strain p25.A12, we grew strains together using a variant of p25.C2 tagged with luciferase (*42*) to measure its relative abundance in three replicates. As a control, we also competed p25.C2 with p25.A12ΔTFA. Five ratios of p25.A12 and p25.C2 were used to determine whether the concentration of the tailocin strain affected killing while controlling the abundance of the target strain. We found that p25.A12 significantly reduced the growth of p25.C2 in the three highest ratios tested (Fig. 3E). The 10:10 and 3:10 ratios significantly differed from the p25.A12ΔTFA competitive assay, suggesting that having a functional tailocin suppresses the growth of p25.C2 and that p25.A12 is no longer able to significantly reduce the growth of p25.C2 when lacking the tailocin. The 5:10 ratio did not significantly differ from the p25.A12ΔTFA competitive assay, perhaps due to technical error. We found that p25.C2 grown with p25.A12ΔTFA was never significantly different from p25.C2 grown alone, suggesting that tailocin is an effective competitive mechanism in the plant host. Additionally, the mutant and wild-type p25.A12 were shown to have no growth differences in planta (fig. S7). These results were replicated in competition assays done in test tubes (fig. S8); however, in these trials, p25.A12ΔTFA competing with p25.C2 significantly differed from the control for the highest ratio. This result could indicate that p25.A12 uses another competitive mechanism in the absence of tailocin, which proves ineffective at lower starting abundances. These results suggest that tailocin killing is important in killing closely related competitors in planta.

### The tail fiber is coevolving with its O-antigen receptor in natural populations

The differences that we observed between strains in their susceptibility to tailocin (Fig. 3B) indicated that these strains may encode an unidentified receptor that has different variants. To identify the receptor, we conducted a transposon mutagenesis screen (*43*) in which we screened a mutant library of a susceptible strain (p25.C2) for insertions that render the strain resistant to the p25.A12 tailocin (Fig. 4A). Insertions (putative knockouts) in 70 genes were significantly associated with resistance to the tailocin. Six of these genes lie within an O-antigen biosynthesis gene cluster, a locus previously implicated in resistance to phage and tailocin tail fibers (*44*, *45*). These results suggested that differences between strains in their O-antigen may explain differences in tailocin susceptibility. Comparative deoxycholic acid (DOC)–PAGE analysis of the lipopolysaccharide (LPS) isolated from two resistant and two susceptible strains showed that the resistant strains lacked the high-molecular-weight polysaccharide chain that was present in the susceptible strains. Subsequent gas chromatography–MS (GC-MS) (Fig. 4C) revealed that the susceptible strains had relatively high amounts of rhamnose compared with the resistant strains (table S2). Our finding of the higher content of rhamnose, along with the expanded size of the LPS in tailocin-resistant strains, agrees with previous studies suggesting that the affected gene locus might be involved in the biosynthesis of the O-antigen in *Pseudomonas* (*46*–*48*). Here, we propose that the O-antigen is likely a receptor for the focal tailocin.

Given that strains are resistant to their own tailocins (*33*), we posited that the tailocin and receptor loci should coevolve. To test this, we measured congruence between tail fiber and LPS haplotypes (Fig. 4B) and found that the tail fiber and LPS haplotypes statistically covaried (Fisher's exact test, $P < 2.72 \times 10^{-10}$ for every association between presence or absence of the gene and the length-based clusters; Fig. 4B). Knowing that the tail fiber haplotype allows for prediction of the LPS haplotype. These experiments support a model in which the tail fiber and LPS of co-occurring *Pseudomonas* strains are evolving in concert in wild *A. thaliana* populations (Fig. 4D).

### The divergent tailocin and LPS haplotypes have been maintained across time and space

To ascertain the time scales of the emergence of the tailocin and different tailocin variants, we sought to retrieve *Pseudomonas* genomes from historical *A. thaliana* herbarium specimens collected over the past two centuries. Only historical *Pseudomonas* genomes can reveal whether extant populations are the result of population continuity or population replacement. We used state-of-the-art ancient DNA retrieval and sequencing techniques (*49*) to sequence leaves of 35 *A. thaliana* herbarium specimens using shotgun genomics (table S3). We mapped the herbarium-derived reads to the ATUE5 reference genome strain to identify *Pseudomonas* reads and found seven samples with >60% of the genome covered by at least one sequencing read (mean genome coverage 0.97 to 8.7x) (fig. S9 and table S3). The *Pseudomonas*-derived reads showed patterns of DNA damage and fragmentation typical of ancient DNA (*50*), which authenticated their historical origin (fig. S10). Our analysis revealed that herbarium specimens preserve the genomes of highly abundant bacterial genera of the *A. thaliana* phyllosphere.

To place the historical *Pseudomonas* genomes in the context of extant genetic diversity, we first used patterns of homozygosity support to identify herbarium specimens most likely to be colonized by a single dominating *Pseudomonas* strain (fig. S11).

This analysis allowed us to select three historical samples (mean genome depth of 8.2 to 9.6x), which we combined with 65 present-day *Pseudomonas* genomes to build a phylogenetic tree using whole-genome single-nucleotide polymorphisms (SNPs). The three historical samples were placed within the present-day ATUE5 diversity (Fig. 5), showing the genetic continuity of this clade for at least the past 177 years. Moreover, the mappings of the historical samples against the ATUE5 reference genome identified the presence of the tailocin in all three historical bacterial genomes (Fig. 5A). To ascertain the tailocin variants encoded in the historical genomes and to assess whether

ERRATUM PUBLISHED 10 APRIL 2025; SEE LAST PAGE



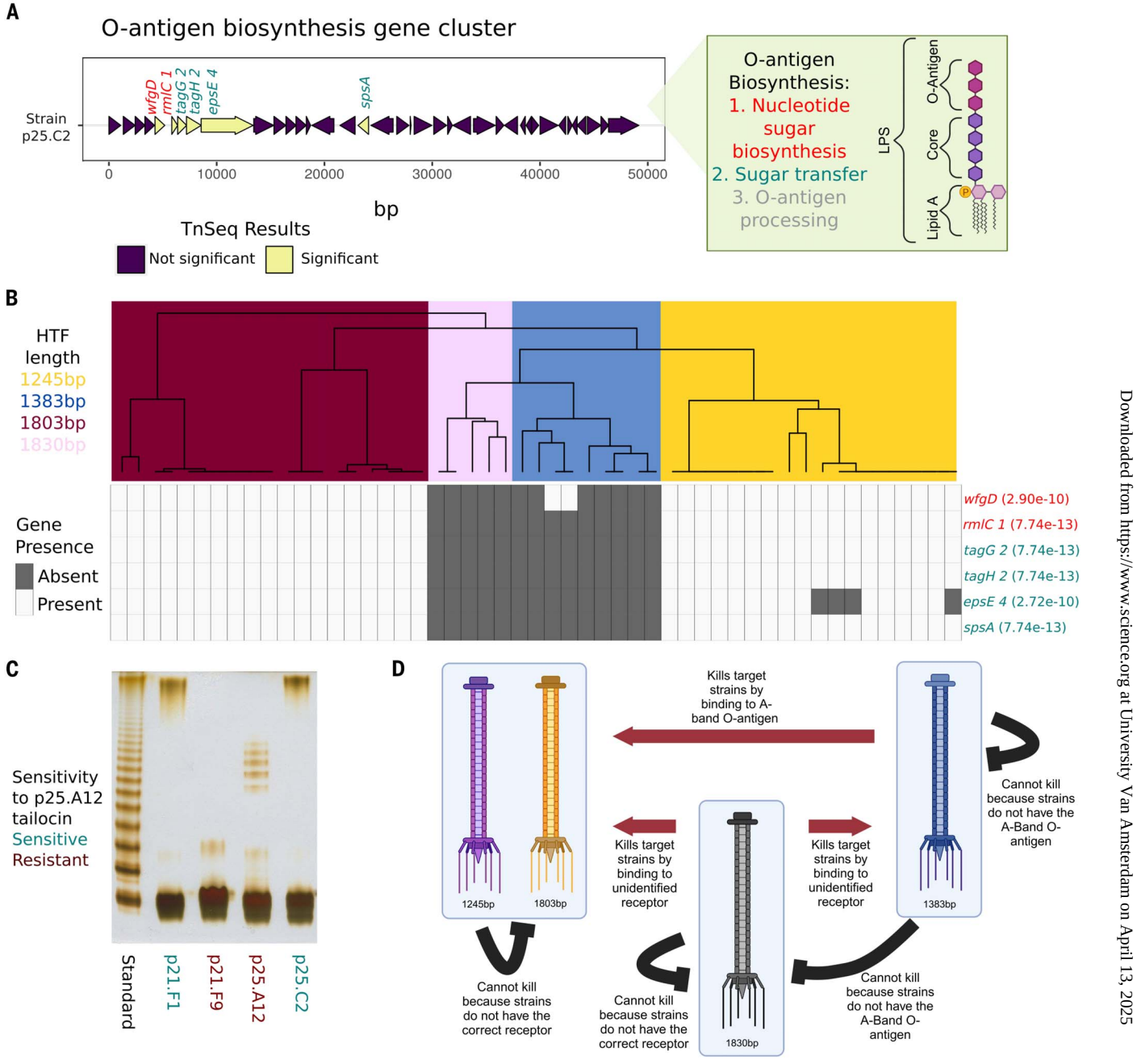


**Fig. 4. The O-antigen is important for tailocin lethality and is coevolving with the tailocin HTFP.** (**A**) Gene plot of the previously characterized O-antigen gene cluster found in the ATUE5 strains. Six of the 70 significant TnSeq genes in this study were found in this gene cluster and are shown in yellow. Gene names are colored by the step in the O-antigen biosynthesis pathway. (**B**) The top dendrogram is from hierarchical clustering of the PanKmer (*92*) output for the hypothetical tail fiber gene and colored by length. Rows represent the six significant O-antigen genes. Gray corresponds to gene presence and white to gene absence. Fisher's exact test *P* values between genes and length-based clusters are shown in parentheses. (**C**) DOC-PAGE profile of silver-stained LPS (1 μg each lane) isolated from a subset of ATUE5 strains. The standard is of *Salmonella enterica* Ser. *typhimurium* (S-type LPS). Gray boxes indicate the high-molecular-weight O-chain. (**D**) Our working model of tailocin killing and lethality in *P. viridiflava* isolates. Red arrows indicate known significant patterns of killing. Black lines show known significant patterns of nonkilling. [Figure created with BioRender.com].

the gene colinearity and the insertion location in the bacterial genome are conserved in the historical genomes, we performed de novo assembly of historical *Pseudomonas*-derived reads. We obtained an average of nine contigs per sample (average sequence length of ~3.4 kb) that were sufficient to show that both the insertion place of the tailocin and the colinearity of its genes are conserved in the historical genomes (Fig. 5A). Moreover, we ascertained that each historical genome carries a different tailocin variant and that all historic variants are segregating in present-day populations (Fig. 5B and fig. S12A). The polyphyletic distribution of the *HTF* and *TFA* gene haplotypes (Fig. 5B and fig. S12A) is likely the result of recombination at this locus (*40*).

We used our phylogenetic reconstruction to determine that the tail fiber assembly gene

ERRATUM PUBLISHED 10 APRIL 2025; SEE LAST PAGE



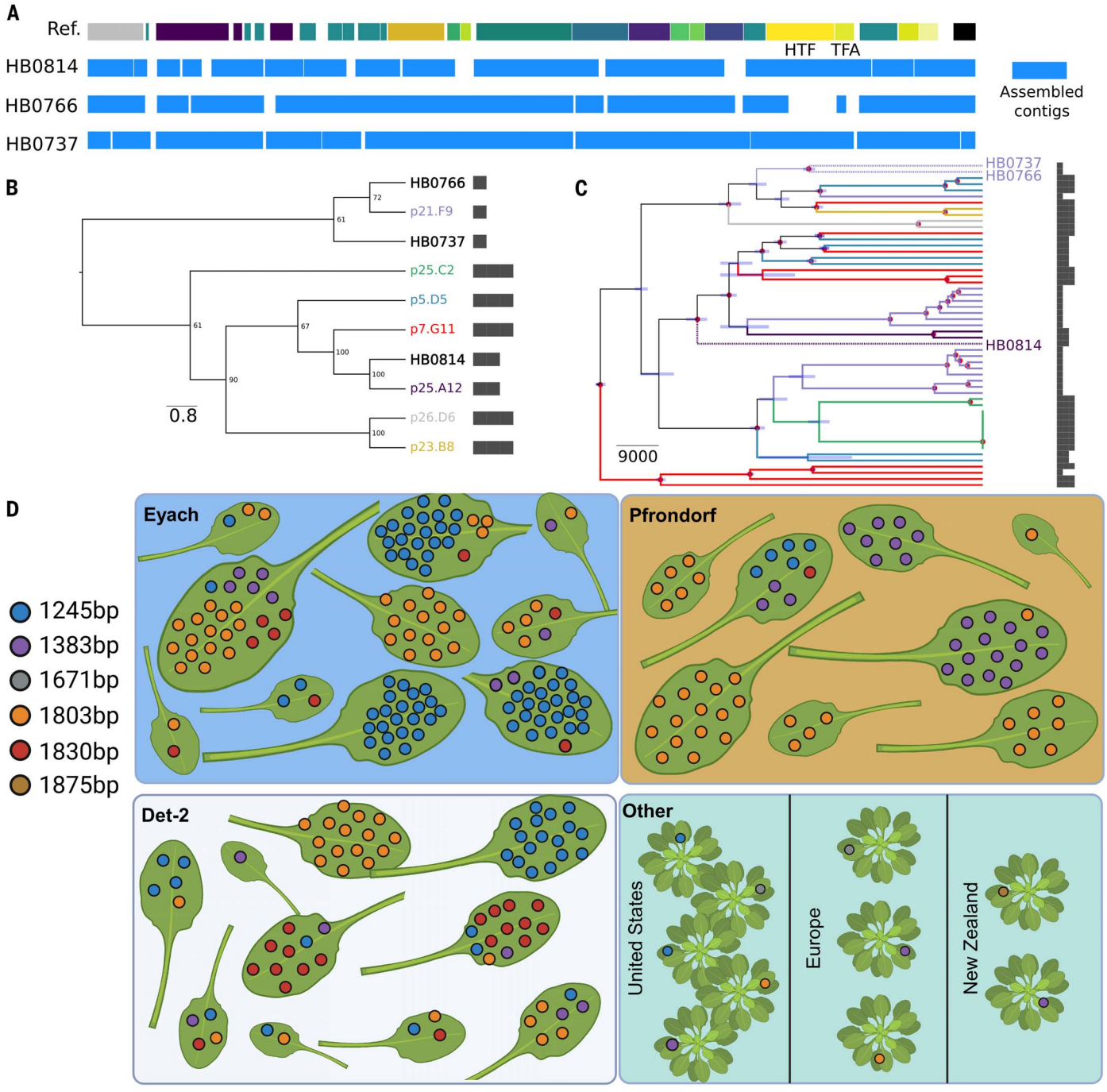


**Fig. 5. The same length haplotypes of HTF are present in contemporary and century-old historical samples, and the HTF haplotype diversity is maintained at the leaf scale and broader geographical scales.** (**A**) De novo assembled contigs spanning the tailocin genomic region for the historical samples. The reference track on the top represents the genes present in the ATUE5 reference genome. The blue boxes depict the de novo assembled contigs. (**B**) Maximum-likelihood neighbor-joining tree of the *HTF* gene translated sequence. Historical samples (HB) are placed in the context of the most common haplotypes. HTF lengths are shown with bars. (**C**) Bayesian tip-date calibrated phylogeny representing the evolutionary relationship between historical and modern *Pseudomonas* strains. The tips and branches are colored based on the *HTF* gene haplotype. Only historical sample labels are shown with stars. The node bars represent the 95% highest posterior density intervals of the estimated time, and the nodes marked with red dots represent those with a posterior probability of 1. HTF lengths are shown with bars. (**D**) A subset of eight to 10 plants from the three German populations (blue, orange, and white panels) and 10 *P. syringae* isolates collected from plants globally, which were downloaded from NCBI (green). Each leaf is from a single plant. Colored dots indicate a single bacterial isolate found and its corresponding HTF length. Plants in the bottom right panel indicate those not found within the same population. [Figure created with BioRender.com]

haplotypes of the historical genomes are closely related to different modern haplotypes (Fig. 5C and fig. S12B), suggesting that the same haplotypes have circulated in the *Pseudomonas* metapopulation for the past 177 years.

The observed persistence of HTF length haplotypes within the bacterial metapopulation may result from a potential artifact introduced by population structure at the plant, plant patch, or site level. At these levels, specific haplotypes could reach fixation, creating the appearance of the maintenance of multiple haplotypes when analyzing all populations collectively. To rule out this possibility, we looked at the co-occurrence of the HTF length haplotypes at the level of single leaves, all collected within a single site in the German metapopulation, as well as at broader geographic locations using 10 *P. syringae* genomes from the National Center for Biotechnology Information (NCBI) (five isolates collected from the US, three from Europe, and two from New Zealand). We found that HTF lengths co-occurred in single leaves and in all three German populations (Fig. 5D). Additionally, we found that the 1245-, 1383-, and 1803-bp HTF lengths in isolates from other countries, in addition to two other lengths. These results suggest that HTF lengths are conserved and maintained at the microscale and over great geographic distances.

## Discussion

We discovered that a tailocin, or repurposed phage, is conserved as part of the core genome of metapopulations of the pathogen *P. viridiflava*. The sequence conservation of its genes (other than *TFA* and *HTF*) indicates that the tailocin is likely essential for survival in *P. viridiflava* pathogen metapopulations. This finding is consistent with previous work suggesting that antimicrobial nanomachines such as the type VI secretion system are important for survival in the plant environment (*51*). Despite the conservation of the entire tailocin gene cluster, multiple allelic variants of the tailocin have been maintained in these populations. We found that the allelic variants target different strains of related pathogenic *P. viridiflava* that differ in the LPS-enriched outer leaflet of the outer membrane (*28*). Similar to the coevolution of toxin-antitoxin systems, the tail fiber and assembly proteins of an ATUE5 strain are coevolving with the LPS membrane composition (*52*). The strong evolutionary conservation and correlation between loci suggests that inter-*Pseudomonas* strain competition through the tailocin is a strong and persistent selective pressure on *Pseudomonas* pathogens.

Second, our results showed that the same tail fiber and/or LPS variants have been maintained in the *Pseudomonas* populations for the past 200 years. Bacteria are capable of rapid adaptation (*53*). The fact that a defined set of variants was maintained in these populations indicates selective constraints on the evolution of this system, consistent with what has been found in viral evolution (*54*). The presence of a limited set of tail fiber haplotypes in the metapopulation could reflect a limited panel of resistance mechanisms.

Our findings provide a roadmap for identifying tail fiber specificities to different strains and introduce the possibility of determining the mechanism of this specificity. Tailocin therapy, like phage therapy, has been proposed as a possible alternative to small-molecule antibiotics (*12*, *13*, *55*). Proof-of-concept studies have shown that tailocins can be used to suppress specific pathogens in animal (*55*) and plant (*12*) models. With any antimicrobial treatment, there is a risk that the target bacterium will evolve resistance. Our findings indicate that, considering the probable constrained array of resistance mechanisms, the tailocin genetic diversity of a pathogen metapopulation can be mined to discover "tailocin cocktails." These cocktails have the potential to target the metapopulation in parallel, thereby reducing the likelihood of resistance evolution. In the future, the mining and characterization of the tailocin repertoire from diverse wild *Pseudomonas* populations should unveil possible combinations between the tail fiber and LPS composition, as well as the time scales in natural settings over which tailocin resistance emerges.

## Materials and Methods

### Bacterial strains, plasmids, and growth conditions

The strains used in this study are detailed in table S2. Bacteria were grown on nutrient lysogeny broth (LB) agar and in nutrient LB medium at 28°C for *Pseudomonas* strains and at 37°C for *Escherichia coli* strains. All liquid cultures were incubated with shaking at 180 rpm. Growth media were supplemented with kanamycin (50 mg/ml, Km50), nitrofurantoin (100 mg/ml, NFN100), or tetracycline (20 mg/ml, TET20). All strains were stored at −80°C in 20% glycerol [v/v]. For plasmid preparation, *E. coli* transformants were cultured in LB. TET20 was used to select *E. coli* transformants. LB supplemented with sucrose, and nitrofurantoin (10 g/L tryptone, 5 g/L yeast extract, 10% w/v filtered sucrose, 15 g/L agar, NFN100) plates were used in the selection of the second *P. syringae* homologous recombination event.

### Viral identification and clustering

*VIBRANT* v1.2.1 (*24*) was run on the 1524 assembled *Pseudomonas* genomes and 10 NCBI genomes to identify viral sequences. To group the 3104 annotated viral sequences from *VIBRANT* into genetically similar clusters, the pairwise mutation distance was calculated for all 3104 viral sequences with Mash v2.2.2 (*27*), a MinHash-based technique that reduces sequences to compressed k-mer representations (sketches). Mash was run ignoring single-copy k-mers that are more likely the result of sequencing errors, and a sketch size of 10,000, which corresponds to the number of nonredundant MinHash values that are kept for the pairwise distance calculation. This resulted in a 3104 × 3104 pairwise mutation distance matrix. Next, the viral sequences were clustered from the pairwise mutation distance matrix with principal component analysis and k-means clustering (*56*, *57*). Silhouette analysis (*58*) was performed to determine the optimal number of clusters for the data.

### Annotation of the VC2 gene cluster

A highly conserved viral sequence, the VC2 gene cluster, was identified in assembled genomes using VIBRANT v1.2.1, and groups of orthologous genes (orthogroups) were identified using *panX* (*59*). Insertion sites for VC2 gene clusters were identified by searching for orthologs of the known viral sequence flanking genes *mutS*, *cinA*, *trpE*, and *trpG*. VC2 was always found between *trpE* and *trpG*. Gene function predictions were determined by orthologous viral genes previously characterized in *VIBRANT* and *BLAST*. Tailocin gene clusters were visualized with the R package "gggenes."

### Viral particle extraction and partial purification

Overnight cultures were back-diluted into 50 ml of fresh LB to extract and isolate tailocins from the various *Pseudomonas* strains. When cultures reached an exponential growth phase [an optical density at 600 nm ($OD_{600}$) of 0.4 to 0.6), 5 μg/ml MMC (Selleck, catalog no. S8146) was added to induce the bacterial SOS (Save-Our-Soul) response and tailocin induction. The cultures were then incubated at 28°C for a minimum of 18 hours and then centrifuged at 4°C for 1 hour at 1400 × *g* to pellet cell debris. The supernatants were sterilized by filtration with 0.2-μm cellulose acetate filters. To precipitate viral particles, 40% (w/v) of ammonium sulfate was slowly added to the filter-sterilized tailocin lysate while stirring on ice. The lysate was left stirring on ice for at least 18 hours. After 18 hours at 4°C, the ammonium sulfate was pelleted by centrifugation at 2090 × *g* for 2 hours at 4°C. The supernatant was discarded and the pellet was resuspended in 500 μl of cold P-buffer (100 mM NaCl, 8 mM $MgSO_4$, 50 mM Tris-HCl, pH 7.5) and stored at 4°C. Tailocin lysates were used fresh or for up to 2 weeks.

### Visualization of viral particles using TEM

One negatively stained specimen (from strain p25.A12) was prepared and imaged in the following manner. First, 3.5 μl of sample was placed on a carbon-coated, TEM grid that had been glow discharged to make it more hydrophilic. After ~1 min, filter paper was used to remove excess solution from the grid by touching

the side of the grid. This was followed by two steps of brief (~1 to 2 s) washing in P-buffer and blotting with filter paper in the same manner. Next, this process was repeated twice but with the negative stain solution (1% ammonium molybdate). Finally, the grid was incubated for 15 to 20 s in a droplet of 1% ammonium molybdate, blotted again, and allowed to air dry. Negatively stained specimens were viewed on Tecnai 12 (ThermoFisher Scientific, Waltham, MA) and JEM-1400 (JEOL, Tokyo, Japan) transmission electron microscopes operated at 120 kV. Images were recorded on an UltraScan and Orius cameras (Gatan, Pleasanton, CA) respectively.

### MS characterization of tailocin proteins

Tailocins partially purified as described above were treated with or without MMC and resuspended in 50 mM triethylammonium bicarbonate and 5% SDS (1× S-TRAP buffer) and frozen at −80°C until digestion. Total protein content was quantified using the Pierce BCA Protein Assay Kit (ThermoFisher Scientific), and 10 μg of protein was diluted into 25 μl of 1× S-TRAP buffer. The protein was reduced with 20 mM dithiothreitol at 37°C for 30 min and alkylated with 40 mM iodoacetamide at room temperature for 45 min in the dark. Samples were acidified with phosphoric acid and digested using micro-S-TRAP columns (Protifi, Fairport, NY) with 0.5 μg of trypsin/Lys C per sample according to the manufacturer's instructions. The peptides were dried to completion, resuspended in 300 μl of 0.1% trifluoroacetic acid, and desalted using Pierce Peptide Desalting Spin Columns (ThermoFisher Scientific) according to the manufacturer's instructions. The peptides were resuspended in 40 μl of 0.1% formic acid for LC-MS/MS analysis.

Reversed-phase nano-LC-MS/MS was performed on an Dionex UltiMate 3000 RSLCnano system coupled to a ThermoFisher Scientific Q Exactive-HF orbitrap mass spectrometer equipped with a nanoelectrospray source. One microgram of each sample was first trapped on a 2-cm Acclaim PepMap-100 column (ThermoFisher Scientific) with 5% acetonitrile at 5 μl/min. Then at 5 min, the sample was injected onto the LC reverse-phase Acclaim PepMap 100 C18 2.0 μm nanocolumn (ThermoFisher Scientific). A 500-mm-long, 0.075-mm inner-diameter nanocolumn heated to 35°C was used for chromatographic separation. The peptides were eluted with a gradient of reversed-phase buffers (buffer A: 0.1% formic acid in water; buffer B: 0.1% formic acid in 100% acetonitrile) at a flow rate of 0.2 μl/min. The LC run lasted for 85 min with a starting concentration of 5% buffer B, increasing to 28% buffer B over 75 min, up to 40% buffer B over 10 min, and held at 90% buffer B for 10 min. The column was allowed to equilibrate at 5% buffer B for 20 min before starting the next data acquisition. The Q Exactive-HF mass spectrometer was operated in data-dependent acquisition MS/MS analysis mode selecting the top 20 most abundant precursor ions between 375 and 1650 $m/z$ at 60,000 resolution for fragmentation at 15,000 resolution.

The raw data were analyzed using Proteome Discoverer 3.0 software with the SEQUEST algorithm against the uniprot_ref_pseudomonas_viridiflava database (1-18-2023 version with 4389 proteins) or the p25.A12 database. An allowance was made for two missed cleavages after trypsin and Lys C digestion. No fixed modifications were considered. The variable modifications of methionine oxidation and cysteine carbamidomethylation were considered with a mass tolerance of 15 ppm for precursor ions and a mass tolerance of 0.02 Da for fragment ions. The results were filtered with a false discovery rate of 0.01. A minimum of one unique peptide was reported for all proteins identified.

### Allelic diversity and nucleotide sequence data analysis

Orthogroups that were previously identified using panX were included in the analysis. The nucleotide and peptide sequences were aligned with Clustal Omega (*60*), and then a codon-based nucleic acid alignment was generated with pal2nal (*61*). This step is critical to ensure that the nucleic acid alignment is aligned codon by codon to determine whether substitutions result in a synonymous or nonsynonymous amino acid change. The output aligned file was saved in fasta format and used as an input file for population summary statistic calculations in R using the package PopGenome v2.7.5 (*62*). The level of sequence diversity among ortho groups was compared using the summary statistics $\pi$ (average pairwise difference or average number of nucleotide diversity per site) (*63*) and $\theta$ (population mutation parameter or number of segregating sites) (*64*), whereas Tajima's D (*65*) was used as a proxy for the SFS, and thus to determine the demographic and selective forces shaping the SFS of tailocin genes.

### Ascertainment of tailocin haplotypes

To determine how many haplotypes of tail fiber assembly and hypothetical tail fiber genes there are in the pathogenic strains in our study, nucleotide and peptide alignments from Clustal Omega (*60*) were analyzed using the R package pegas (*66*). The haplotype function was used to determine how many unique haplotypes are in the ATUE5 strains. The most common haplotypes were used for downstream analyses.

### Mapping of reads from historical samples to ATUE5

A set of 35 herbarium *A. thaliana* samples collected between 1817 and 1957 from southern Germany (table S3) (*67*) were screened for *Pseudomonas* presence. Adapter sequences from the raw reads were trimmed and merged using Adapterremoval V.2 (*68*) and subsequently mapped to the *Pseudomonas* p25.A12 assembly using bwa aln v.0.7.17 (*69*) with seed deactivation to allow the alignment of of substitutions present at the termini of the reads, for example, those arising from DNA deamination in historic material (*49*). A total of seven samples for which the *Pseudomonas* reference genome was covered in at least 60% were kept (table S2). To authenticate the historic origin of the bacterial reads, the proportion of C-to-T (or G-to-A) substitutions, as well as the fragment size distribution of the reads, were computed using mapDamage v.2.2.1 (*70*) (fig. S8). Patterns of homozygosity in the mapped reads were analyzed and only samples that were likely dominated by single *Pseudomonas* lineages were retained (fig. S10). As a result, only the samples HB0737, HB0766, and HB0814 were kept for downstream analyses.

### Ascertainment of tailocin variants in historical genomes

To identify reads aligning to the whole spectrum of tailocin genetic diversity, different haplotypes of the highly polymorphic tail fiber assembly and hypothetical tail fiber genes (Fig. 3A) were added to the p25.A12 reference genome before the historical samples were mapped as described above. Reads covering the Tailocin region surrounded by the flanking genes *trpE* and *trpG*, as well as all reads covering any haplotype of the mentioned genes, were subset from the raw reads and used as input for de novo assembly using SPAdes v.3.13.0 (*71*). Samples HB0737, HB0766, and HB0814 yielded 10, 9, and 14 assembled contigs, respectively (table S4). To find collinearity between the de novo assemblies and the reference Tailocin region, we used minimap v.2.1 (*72*). Amino acid–translated sequences of the historical isolate–specific haplotypes for the tail fiber assembly protein and putative tail fiber protein were merged together with the haplotypes segregating in the observed diversity. Finally, Clustal Omega v.1.2.4 (*73*) was used to generate a multiple alignment and to classify the haplotypes in the historical samples.

### Whole-genome phylogenetic reconstruction combining present-day and historical genomes

A set consisting of 50 ATUE5 modern and three historic *Pseudomonas* strains was used to create a phylogenetic reconstruction. We used the mapped reads to perform individual de novo variant callings using bcftools mpileup and bcftools call v1.11 (*74*) removing those reads with mapping quality values lower than 30. We then merged all individual calls using bcftools merge v.1.11 (*74*) and removed those samples

with <60% of the called variants. We kept only biallelic SNPs and sites with a maximum missing information of 10% of the remaining samples. The number of retrieved variants were 176,528 SNPs segregating among 53 strains (50 modern and three historic).

Using the genomic SNPs, we sought to reconstruct the phylogenetic relations among the 53 strains. We used IQ-TREE V2.2.0.3 (*75*) in combination with ModelFinder (*76*), and ultrafast bootstrap UFBoot (*77*) to estimate a maximum-likelihood phylogenetic tree. Variant sites that are likely to arise due to putative recombination were identified using ClonalFrameML v.1.12 (*78*), and the output was used to mask putative recombinant positions in the original genomic SNP array. BEAST2 (*79*) was used to jointly estimate the phylogenetic relations among the strains and the relative time of emergence for all the tree nodes. For this purpose, we used the collection dates (table S3) and a previously estimated evolutionary rate (*80*) as priors. To minimize parameter estimation, we chose HYK as the evolutionary model, and to avoid demographic history assumptions, we used a coalescent extended Bayesian skyline approach (*81*).

### *Testing bacterial sensitivity to tailocins with spot test phenotypic assays*

To test the sensitivity of the different bacterial strains to the tailocins, soft agar assays were performed using an adaptation of a protocol from Vacheron *et al*. (*41*). Overnight cultures (750 µl) of each strain were mixed with 25 ml of LB soft agar (0.8%), and the mixture was poured into a square plate and left to harden. Then, aliquots of 3 to 5 µl of concentrated viral particles suspension were applied to the agar, along with a control of P-buffer alone and noninduced cultures in serial dilutions. The plates were incubated overnight at 30°C. Bacterial sensitivity or resistance to the viral particles was assessed after 24 hours. When testing serially diluted tailocins, no plaques were observed, suggesting that the killing agent is nonreplicative and not a phage. When testing the uninduced tailocin control samples (not induced with mitomycin C), if lethality was observed, the interaction was deemed to be inconclusive. Spot tests were performed in three biological and three technical triplicates.

### *Testing bacterial sensitivity to tailocins in culture*

To test the sensitivity of a known sensitive strain (p25.C2) to the mutant tailocin from 25.A12ΔTFA, p25.C2 was grown overnight and then diluted by a factor of 1:10 in fresh LB medium. Once the culture reached the growth phase, cultures were supplemented with 5% p25.A12 tailocin, 5% p25.A12ΔTFA tailocin, or a buffer control. $OD_{600}$ was measured in a 96-well plate using a microplate reader (TECAN Spark).

### *Construction of the* Pseudomonas *p25.A12 tail fiber assembly gene deletion*

The p25.A12ΔTFA mutant strain was cloned using the Gateway cloning system with the donor vector pDONR1K18ms (Addgene plasmid no. 72644) and the destination vector pDEST2T18ms (Addgene plasmid no. 72647). Briefly, the upstream and downstream sequences of the TFA were amplified using primers with 5′-end sequences identical to the *att*B sites of a suicide plasmid (table S4). The polymerase chain reaction (PCR) products were analyzed by gel electrophoresis and purified with the GeneJET gel extraction kit (ThermoFisher Scientific, catalog no. K0691). BP and LR reactions were conducted in the one-tube format using the purified *att*B-flanked PCR product. The resulting expression clone was transformed into competent *E. coli* DH5α and then introduced into recipient cells (*P. viridiflava* p25.A12) by conjugation. Recombinant cells (merodiploids) were selected for with the antibiotic resistance conferred by the expression clone and verified with PCR and gel electrophoresis. Positive colonies were purified by streaking onto new plates. Purified merodiploids were grown overnight without the antibiotic conferred by the expression clone to allow for another recombination event and then plated on 10% D-sucrose for *sacB* counterselection. Colonies were examined by PCR and verified by DNA sequencing (GeneWiz).

### *Construction of the* Pseudomonas *p25.A12 tail fiber assembly gene overexpression rescue vector*

The *HTF* gene was cloned into pMCSG11 (*82*) by restriction cloning (*83*). This rescue vector was transformed into p25.A12ΔTFA, tailocins were induced and partially purified, and killing assays were performed to assess rescue lethality.

### *Plant infections of wild-type or mutant strains*

To evaluate the infection outcome of p25.A12 wild type and mutant (p25.A12ΔTFA), Columbia-0 wild-type *A. thaliana* plants were grown under long-day conditions (16 hours light, 8 hours dark) in an AR41L3 Percival detector with 60% intensity of the SciWhite LED lights. Seedlings were grown in 24-well plates (Greiner Bio-One, catalog no. 6621665). Thirteen-day-old seedlings were used for the infections. Plants were infected with bacterial suspension of the *P. viridiflava* strain p25.A12, p25.A12ΔTFA, or buffer (10 mM $MgSO_4$). Both p25.A12 strains were tagged with luciferase (*42*).

Bacteria were grown overnight and diluted 1:10 the day of the infection. Cells were grown for another 3 hours and then collected and resuspended in 10 mM $MgSO_4$ to a final $OD_{600}$ of 0.01. A 200-µl sample was used to spot inoculate the plants in a randomized manner. Plants were grown for 7 days and then collected. The collected plants were ground in 1 ml of 10 mM $MgSO_4$ using the Qiagen tissue lyser II, and 200 µl of the suspension was used to measure luciferase in the TECAN using flat white plates (TECAN, catalog no. 30122300). Plants infected with $MgSO_4$ were used as controls. In total, 24 plants were used for each strain or buffer.

### *In vitro competition assays*

Strain p25.C2 cultures tagged with a luciferase cassette were grown together with p25.A12 wild type or the p25.A12ΔTFA strain. Five different ratios were used for mixing the two strains (10:10, 5:10, 3:10, 2:10, and 1:10) keeping the p25.C2 strain constant at a final $OD_{600}$ of 0.005. Bacteria were grown overnight and then diluted 1:10 the day of the experiment. Cells were grown for another 3 hours with shaking and then collected and mixed accordingly. The co-inoculated cells were grown in a TECAN flat white plate (TECAN, catalog no. 30122300) in a final volume of 200 µl in a randomized manner. The plates were placed in the TECAN plate reader (TECAN Spark) for 21 hours at 28°C for 55 kinetic cycles. Each cycle consisted of 15 min or orbital shaking at 220 rpm, resting for 5 min, and then measuring the luciferase-tagged p25.C2 cells in each well. For the analysis, the three highest values from each sample were used, and the average luciferase value was calculated for each condition.

### *In planta coinfections*

Columbia-0 wild-type *A. thaliana* plants were grown in 24-well plates (Greiner Bio-One, catalog no. 6621665) under long-day conditions (16 hours light, 8 hours dark) in an AR41L3 Percival detector with 60% intensity of the SciWhite LED lights. Thirteen-day-old seedlings were used for the infections. Plants were infected with bacterial suspension of the *Pseudomonas* strain p25.C2 (tagged with luciferase) and either the p25.A12 wild type or the p25.A12ΔTFA strain. The same five ratios as the in vitro assays were used, keeping the p25.C2 constant at a final $OD_{600}$ of 0.005.

Bacteria were grown overnight and diluted 1:10 the day of the infection. Cells were grown for another 3 hours and then collected and resuspended in 10 mM $MgSO_4$. Cells were then mixed according to the ratios described above, and the seedlings were submerged in 10 ml of cell suspension for 10 min in a randomized manner. Sampls of 850 µl were removed and the plants were placed back in the AR41L3 Percival detector. Three days after infection, plants were collected in 2-ml deep-well plates (Thermo Fisher Nunc, catalog no. 12-565-605) containing 1 ml of $MgSO_4$. Plants

were ground using the Qiagen tissue lyser II, and 200 µl of the suspension was used to measure luciferase in the TECAN using flat white plates (TECAN, catalog no. 30122300). Plants infected with $MgSO_4$ or p25.C2 alone were used as controls. Each treatment was done in 12 replicates. The entire experiment was repeated three times with similar results.

### Constructing the BarSeq mutant fitness library

Methods were adapted from Wetmore *et al.* (*43*). Briefly, we created the p25.C2 transposon mutant library by conjugating p25.C2 with the *E. coli* conjugation donor (WM3064) harboring the pHLL250 mariner transposon vector library (AMD290) (*84*). Equal cell numbers of mid-log-phase p25.C2 and AMD290 were conjugated for 6 hours on 0.45-µm nitrocellulose filters (Millipore) overlaid on LB agar plates containing diaminopimelic acid. The resuspended cells were plated on LB plates with 50 g/ml kanamycin to select for mutants. After 2 days, the kanamycin-resistant colonies were scraped into LB, the $OD_{600}$ of the mixture was measured, and the mutant library was diluted to a starting $OD_{600}$ of 0.2 in 250 ml of LB with 50 g/ml kanamycin. The diluted mutant library was grown at 28°C to a final $OD_{600}$ of 1.0, glycerol was added to a final volume of 10%, and samples were stored at −80°C as freezer stocks. Cells were then collected for genomic DNA extraction.

### Competitive mutant fitness assays

Assays were adapted from Carim *et al.* (*28*). Briefly, assays were performed in glass tubes. Partially purified tailocins were used as stressors at final concentrations of 0.05× of the stock preparation. P-buffer was used as a control. LB and Km50 was supplied for the mutant library as the growth medium. The tubes were incubated with shaking and mutants were harvested when the $OD_{600}$ reached the mid-log phase. Cells were pelleted by centrifugation (8000 × *g* for 5 min) and stored at −20°C to await genomic DNA extraction. Each condition was assayed in 10 individual replicates.

### BarSeq and analysis of BarSeq data

Genomic DNA was extracted and barcode PCR was performed as described in Wetmore *et al.* (*43*). DNA extractions were quantified with NanoDrop 1000 (ThermoFisher Scientific). Barcode sequence data were obtained by multiplexing on a lane of HiSeq at the University of Utah High-Throughput Genomics core. Fitness data were calculated and analyzed from these reads with the DESeq2 R package (*85*), and scripts can be found on our GitHub page.

### LPS isolation

The cell culture was washed two times with PBS and inactivated using a solution of 1% phenol in PBS. The cell material was suspended in water and preincubated to 68°C with gentle stirring. The extraction was performed by using the corresponding volume of 90% (v/v) liquefied phenol following the standard procedure (*86*) and extracted for 20 min at 68°C. The sample was cooled on an ice bath and centrifuged for 20 min at 4°C, 5000 × *g*. The aqueous upper phase was collected, and the remaining phenol phase and cell debris were extracted two more times with water following the same protocol. The combined aqueous phases and the final phenol phase were dialyzed against several exchanges of water for 4 days 12- to 14-kDa [molecular weight cutoff (MWCO)].

The freeze-dried dialysates were resuspended in a sterile buffer (10 mg/ml to 50 mM $MgCl_2 \cdot 6H_2O$ and 20 mM $NaOAc \cdot 3H_2O$), and the nucleic acids were digested with benzonase (2 µl, 18 hours at 37°C) with gentle agitation. Proteins were digested with proteinase K (50 µg/ml per ml of the LPS solution) by overnight incubation at 37°C. The buffer, nucleotides, and peptides were removed by dialysis against water (12- to 14-kDa MWCO) at 4°C, followed by ultracentrifugation at 100,000 × *g* for 16 hours at 4°C. The LPS pellets were suspended in water and freeze-dried, and were then ready for use.

### DOC-PAGE of LPS samples

The purified LPS samples were resolved in PAGE (4% stacking gel and 18% resolving gel) in the presence of DOC buffer (*87*). The PAGE was visualized with a silver stain reagent kit (Bio-Rad).

### Glycosyl composition analysis using the TMS method

Glycosyl composition analysis was performed by combined GC-MS of the O-trimethylsilyl (TMS) methyl glycoside derivatives produced from the sample by acidic methanolysis followed by trimethylsilylation (*88*). GC-MS analysis of the TMS methyl glycosides was performed on an Agilent AT 7890A GC system interfaced to a 5975B MSD using an Equity-1 (Supelco) fused silica capillary column (30 m length × 0.25 mm ID × 0.25 µm film thickness). The temperature gradient was was 80°C for 2 min, increased to 140°C at 20°C/min with a 2-min hold, increased to 200°C at 2°C/min, and then increased to 250°C at 30°C/min with 5-min hold.

## REFERENCES AND NOTES


1. E. M. Goss, S. Timilsina, A bacterial epidemic in wild plants. *Nat. Ecol. Evol.* **2**, 1529–1530 (2018). doi: 10.1038/s41559-018-0692-2; pmid: 30224816
2. T. L. Karasov *et al.*, *Arabidopsis thaliana* and *Pseudomonas* pathogens exhibit stable associations over evolutionary timescales. *Cell Host Microbe* **24**, 168–179.e4 (2018). doi: 10.1016/j.chom.2018.06.011; pmid: 30001519
3. E. A. Van Der Biezen, J. D. Jones, Plant disease-resistance proteins and the gene-for-gene concept. *Trends Biochem. Sci.* **23**, 454–456 (1998). doi: 10.1016/S0968-0004(98)01311-5; pmid: 9868361
4. T. Ruiz-Bedoya, P. W. Wang, D. Desveaux, D. S. Guttman, Cooperative virulence via the collective action of secreted pathogen effectors. *Nat. Microbiol.* **8**, 640–650 (2023). doi: 10.1038/s41564-023-01328-8; pmid: 36782026
5. P. G. Leiman *et al.*, Type VI secretion apparatus and phage tail-associated protein complexes share a common evolutionary origin. *Proc. Natl. Acad. Sci. U.S.A.* **106**, 4154–4159 (2009). doi: 10.1073/pnas.0813360106; pmid: 19251641
6. C. M. Heiman, J. Vacheron, C. Keel, Evolutionary and ecological role of extracellular contractile injection systems: From threat to weapon. *Front. Microbiol.* **14**, 1264877 (2023). doi: 10.3389/fmicb.2023.1264877; pmid: 37886057
7. T. G. Dong, B. T. Ho, D. R. Yoder-Himes, J. J. Mekalanos, Identification of T6SS-dependent effector and immunity proteins by Tn-seq in *Vibrio cholerae*. *Proc. Natl. Acad. Sci. U.S.A.* **110**, 2623–2628 (2013). doi: 10.1073/pnas.1222783110; pmid: 23362380
8. P. F. Sarris, E. D. Ladoukakis, N. J. Panopoulos, E. V. Scoulica, A phage tail-derived element with wide distribution among both prokaryotic domains: A comparative genomic and phylogenetic study. *Genome Biol. Evol.* **6**, 1739–1747 (2014). doi: 10.1093/gbe/evu136; pmid: 25015235
9. E. T. Granato, T. A. Meiller-Legrand, K. R. Foster, The evolution and ecology of bacterial warfare. *Curr. Biol.* **29**, R521–R537 (2019). doi: 10.1016/j.cub.2019.04.024; pmid: 31163166
10. L. Chen *et al.*, Genome-wide Identification and Characterization of a Superfamily of Bacterial Extracellular Contractile Injection Systems. *Cell Rep.* **29**, 511–521.e2 (2019). doi: 10.1016/j.celrep.2019.08.096; pmid: 31597107
11. A. M. Geller *et al.*, The extracellular contractile injection system is enriched in environmental microbes and associates with numerous toxins. *Nat. Commun.* **12**, 3743 (2021). doi: 10.1038/s41467-021-23777-7; pmid: 34145238
12. A. Príncipe, M. Fernandez, M. Torasso, A. Godino, S. Fischer, Effectiveness of tailocins produced by Pseudomonas fluorescens SF4c in controlling the bacterial-spot disease in tomatoes caused by Xanthomonas vesicatoria. *Microbiol. Res.* **212-213**, 94–102 (2018). doi: 10.1016/j.micres.2018.05.010; pmid: 29853172
13. D. A. Baltrus *et al.*, Prophylactic application of tailocins prevents infection by *Pseudomonas syringae*. *Phytopathology* **112**, 561–566 (2022). doi: 10.1094/PHYTO-06-21-0269-R; pmid: 34320833
14. H. Rasoamanana *et al.*, Bacteriocin production correlates with epidemiological prevalence of phylotype I sequevar 18 *Ralstonia pseudosolanacearum* in Madagascar. *Appl. Environ. Microbiol.* **89**, e0163222 (2023). doi: 10.1128/aem.01632-22; pmid: 36602304
15. R. J. Dorosky, J. M. Yu, L. S. Pierson 3rd, E. A. Pierson, *Pseudomonas chlororaphis* produces two distinct R-tailocins that contribute to bacterial competition in biofilms and on roots. *Appl. Environ. Microbiol.* **83**, e00706-17 (2017). doi: 10.1128/AEM.00706-17; pmid: 28526791
16. R. J. Dorosky, L. S. Pierson 3rd, E. A. Pierson, *Pseudomonas chlororaphis* produces multiple R-tailocin particles that broaden the killing spectrum and contribute to persistence in rhizosphere communities. *Appl. Environ. Microbiol.* **84**, e01230-18 (2018). doi: 10.1128/AEM.01230-18; pmid: 30030224
17. I. Hanski, Metapopulation dynamics. *Nature* **396**, 41–49 (1998). doi: 10.1038/23876
18. T. L. Karasov *et al.*, The long-term maintenance of a resistance polymorphism through diffuse interactions. *Nature* **512**, 436–440 (2014). doi: 10.1038/nature13439; pmid: 25043057
19. O. Shalev *et al.*, Commensal *Pseudomonas* strains facilitate protective response against pathogens in the host plant. *Nat. Ecol. Evol.* **6**, 383–396 (2022). doi: 10.1038/s41559-022-01673-7; pmid: 35210578
20. D. S. Lundberg *et al.*, Contrasting patterns of microbial dominance in the *Arabidopsis thaliana* phyllosphere. *Proc. Natl. Acad. Sci. U.S.A.* **119**, e2211881119 (2022). doi: 10.1073/pnas.2211881119; pmid: 36538480
21. J. De Smet, H. Hendrix, B. G. Blasdel, K. Danis-Wlodarczyk, R. Lavigne, Pseudomonas predators: Understanding and exploiting phage-host interactions. *Nat. Rev. Microbiol.* **15**, 517–530 (2017). doi: 10.1038/nrmicro.2017.61; pmid: 28649138
22. S. L. Weaver, L. Zhu, S. Ravishankar, M. Clark, D. A. Baltrus, Interspecies killing activity of *Pseudomonas syringae* tailocins. *Microbiology* **168**, mic.0.001258 (2022). pmid: 36342839
23. C. B. Silveira, A. Luque, F. Rohwer, The landscape of lysogeny across microbial community density, diversity and energetics. *Environ. Microbiol.* **23**, 4098–4111 (2021). doi: 10.1111/1462-2920.15640; pmid: 34121301

24. K. Kieft, Z. Zhou, K. Anantharaman, VIBRANT: Automated recovery, annotation and curation of microbial viruses, and evaluation of viral community function from genomic sequences. *Microbiome* **8**, 90 (2020). doi: 10.1186/s40168-020-00867-0; pmid: 32522236
25. K. Jakob *et al*., *Pseudomonas viridiflava* and *P. syringae*—Natural pathogens of *Arabidopsis thaliana*. *Mol. Plant Microbe Interact.* **15**, 1195–1203 (2002). doi: 10.1094/MPMI.2002.15.12.1195; pmid: 12481991
26. T. L. Karasov *et al*., Drought selection on *Arabidopsis* populations and their microbiomes, bioRxiv (2022) p. 2022.04.08.487684.
27. B. D. Ondov *et al*., Mash: Fast genome and metagenome distance estimation using MinHash. *Genome Biol.* **17**, 132 (2016). doi: 10.1186/s13059-016-0997-x; pmid: 27323842
28. S. Carim *et al*., Systematic discovery of pseudomonad genetic factors involved in sensitivity to tailocins. *ISME J.* **15**, 2289–2305 (2021). doi: 10.1038/s41396-021-00921-1; pmid: 33649553
29. K. Nakayama *et al*., The R-type pyocin of *Pseudomonas aeruginosa* is related to P2 phage, and the F-type is related to lambda phage. *Mol. Microbiol.* **38**, 213–231 (2000). doi: 10.1046/j.1365-2958.2000.02135.x; pmid: 11069649
30. W. H. Roos, I. L. Ivanovska, A. Evilevitch, G. J. L. Wuite, Viral capsids: Mechanical characteristics, genome packaging and delivery mechanisms. *Cell. Mol. Life Sci.* **64**, 1484–1497 (2007). doi: 10.1007/s00018-007-6451-1; pmid: 17440680
31. X. Shen *et al*., Functional identification of the DNA packaging terminase from *Pseudomonas aeruginosa* phage PaP3. *Arch. Virol.* **157**, 2133–2141 (2012). doi: 10.1007/s00705-012-1409-5; pmid: 23011306
32. K. L. Hockett, T. Renner, D. A. Baltrus, Independent co-option of a tailed bacteriophage into a killing complex in *Pseudomonas*. *mBio* **6**, e00452 (2015). doi: 10.1128/mBio.00452-15; pmid: 26265717
33. M. G. K. Ghequire, R. De Mot, The tailocin tale: Peeling off phage tails. *Trends Microbiol.* **23**, 587–590 (2015). doi: 10.1016/j.tim.2015.07.011; pmid: 26433692
34. K. L. Hockett, D. A. Baltrus, Use of the soft-agar overlay technique to screen for bacterially produced inhibitory compounds. *J. Vis. Exp.* **119**, 55064 (2017). doi: 10.3791/55064; pmid: 28117830
35. S. I. Ishii, Y. Nishi, F. Egami, The fine structure of a pyocin. *J. Mol. Biol.* **13**, 428–431 (1965). doi: 10.1016/S0022-2836(65)80107-3; pmid: 4956166
36. J. R. Govan, Studies on the pyocins of *Pseudomonas aeruginosa*: Morphology and mode of action of contractile pyocins. *J. Gen. Microbiol.* **80**, 1–15 (1974). doi: 10.1099/00221287-80-1-1; pmid: 4206804
37. T. B. Higerd, C. A. Baechler, R. S. Berk, Morphological studies on relaxed and contracted forms of purified pyocin particles. *J. Bacteriol.* **98**, 1378–1389 (1969). doi: 10.1128/jb.98.3.1378-1389.1969; pmid: 4977989
38. E. C. Schirmer, J. R. Yates 3rd, L. Gerace, MudPIT: A powerful proteomics tool for discovery. *Discov. Med.* **3**, 38–39 (2003). pmid: 20704860
39. D. Medini, C. Donati, H. Tettelin, V. Masignani, R. Rappuoli, The microbial pan-genome. *Curr. Opin. Genet. Dev.* **15**, 589–594 (2005). doi: 10.1016/j.gde.2005.09.006; pmid: 16185861
40. D. A. Baltrus, M. Clark, C. Smith, K. L. Hockett, Localized recombination drives diversification of killing spectra for phage-derived syringacins. *ISME J.* **13**, 237–249 (2019). doi: 10.1038/s41396-018-0261-3; pmid: 30171255
41. J. Vacheron, C. M. Heiman, C. Keel, Live cell dynamics of production, explosive release and killing activity of phage tail-like weapons for *Pseudomonas* kin exclusion. *Commun. Biol.* **4**, 87 (2021). doi: 10.1038/s42003-020-01581-1; pmid: 33469108
42. A. Duque-Jaramillo *et al*., The genetic and physiological basis of *Arabidopsis thaliana* tolerance to *Pseudomonas viridiflava*. *New Phytol.* **240**, 1961–1975 (2023). doi: 10.1111/nph.19241; pmid: 37667565
43. K. M. Wetmore *et al*., Rapid quantification of mutant fitness in diverse bacteria by sequencing randomly bar-coded transposons. *mBio* **6**, e00306–e00315 (2015). doi: 10.1128/mBio.00306-15; pmid: 25968644
44. P. D. Scanlan *et al*., Coevolution with bacteriophages drives genome-wide host evolution and constrains the acquisition of abiotic-beneficial mutations. *Mol. Biol. Evol.* **32**, 1425–1435 (2015). doi: 10.1093/molbev/msv032; pmid: 25681383
45. J. Jayaraman *et al*., Variation at the common polysaccharide antigen locus drives lipopolysaccharide diversity within the *Pseudomonas syringae* species complex. *Environ. Microbiol.* **22**, 5356–5372 (2020). doi: 10.1111/1462-2920.15250; pmid: 32985740
46. D. A. Baltrus, S. Weaver, L. Krings, A. E. Nguyen, Genomic correlates of tailocin sensitivity in *Pseudomonas syringae*. bioRxiv 538177 [Preprint] (2023); https://doi.org/10.1101/2023.04.24.538177.
47. J. D. King, D. Kocíncová, E. L. Westman, J. S. Lam, Review: Lipopolysaccharide biosynthesis in *Pseudomonas aeruginosa*. *Innate Immun.* **15**, 261–312 (2009). doi: 10.1177/1753425909106436; pmid: 19710102
48. T. Köhler, V. Donner, C. van Delden, Lipopolysaccharide as shield and receptor for R-pyocin-mediated killing in *Pseudomonas aeruginosa*. *J. Bacteriol.* **192**, 1921–1928 (2010). doi: 10.1128/JB.01459-09; pmid: 20118263
49. S. M. Latorre, P. L. M. Lang, H. A. Burbano, R. M. Gutaker, Isolation, library preparation, and bioinformatic analysis of historical and ancient plant DNA. *Curr. Protoc. Plant Biol.* **5**, e20121 (2020). doi: 10.1002/cppb.20121; pmid: 33211414
50. C. L. Weiß *et al*., Temporal patterns of damage and decay kinetics of DNA retrieved from plant herbarium specimens. *R. Soc. Open Sci.* **3**, 160239 (2016). doi: 10.1098/rsos.160239; pmid: 27429780
51. P. Bernal, L. P. Allsopp, A. Filloux, M. A. Llamas, The *Pseudomonas putida* T6SS is a plant warden against phytopathogens. *ISME J.* **11**, 972–987 (2017). doi: 10.1038/ismej.2016.169; pmid: 28045455
52. D. J. Rankin, L. A. Turner, J. A. Heinemann, S. P. Brown, The coevolution of toxin and antitoxin genes drives the dynamics of bacterial addiction complexes and intragenomic conflict. *Proc. Biol. Sci.* **279**, 3706–3715 (2012). doi: 10.1098/rspb.2012.0942; pmid: 22787022
53. E. R. Moxon, P. B. Rainey, M. A. Nowak, R. E. Lenski, Adaptive evolution of highly mutable loci in pathogenic bacteria. *Curr. Biol.* **4**, 24–33 (1994). doi: 10.1016/S0960-9822(00)00005-1; pmid: 7922307
54. V. Druelle, R. A. Neher, Reversions to consensus are positively selected in HIV-1 and bias substitution rate estimates. *Virus Evol.* **9**, veac118 (2022). doi: 10.1093/ve/veac118; pmid: 36632482
55. D. Gebhart *et al*., A modified R-type bacteriocin specifically targeting *Clostridium difficile* prevents colonization of mice without affecting gut microbiota diversity. *mBio* **6**, e02368-14 (2015). doi: 10.1128/mBio.02368-14; pmid: 25805733
56. K. Pearson, LIII. On lines and planes of closest fit to systems of points in space. *Lond. Edinb. Dublin Philos. Mag. J. Sci.* **2**, 559–572 (1901). doi: 10.1080/14786440109462720
57. S. Lloyd, Least squares quantization in PCM. *IEEE Trans. Inf. Theory* **28**, 129–137 (1982). doi: 10.1109/TIT.1982.1056489
58. P. J. Rousseeuw, Silhouettes: A graphical aid to the interpretation and validation of cluster analysis. *J. Comput. Appl. Math.* **20**, 53–65 (1987). doi: 10.1016/0377-0427(87)90125-7
59. W. Ding, F. Baumdicker, R. A. Neher, panX: Pan-genome analysis and exploration. *Nucleic Acids Res.* **46**, e5 (2018). doi: 10.1093/nar/gkx977; pmid: 29077859
60. F. Sievers, D. G. Higgins, Clustal Omega for making accurate alignments of many protein sequences. *Protein Sci.* **27**, 135–145 (2018). doi: 10.1002/pro.3290; pmid: 28884485
61. M. Suyama, D. Torrents, P. Bork, PAL2NAL: Robust conversion of protein sequence alignments into the corresponding codon alignments. *Nucleic Acids Res.* **34**, W609–W612 (2006). doi: 10.1093/nar/gkl315; pmid: 16845082
62. B. Pfeifer, U. Wittelsbürger, S. E. Ramos-Onsins, M. J. Lercher, PopGenome: An efficient Swiss army knife for population genomic analyses in R. *Mol. Biol. Evol.* **31**, 1929–1936 (2014). doi: 10.1093/molbev/msu136; pmid: 24739305
63. M. Nei, W. H. Li, Mathematical model for studying genetic variation in terms of restriction endonucleases. *Proc. Natl. Acad. Sci. U.S.A.* **76**, 5269–5273 (1979). doi: 10.1073/pnas.76.10.5269; pmid: 291943
64. Y. X. Fu, Statistical properties of segregating sites. *Theor. Popul. Biol.* **48**, 172–197 (1995). doi: 10.1006/tpbi.1995.1025; pmid: 7482370
65. F. Tajima, Statistical method for testing the neutral mutation hypothesis by DNA polymorphism. *Genetics* **123**, 585–595 (1989). doi: 10.1093/genetics/123.3.585; pmid: 2513255
66. E. Paradis, pegas: An R package for population genetics with an integrated-modular approach. *Bioinformatics* **26**, 419–420 (2010). doi: 10.1093/bioinformatics/btp696; pmid: 20080509
67. S. M. Latorre, P. L. M. Lang, H. A. Burbano, Historical *Arabidopsis thaliana* genomes from Germany, Zenodo (2022); https://zenodo.org/record/7156189.
68. M. Schubert, S. Lindgreen, L. Orlando, AdapterRemoval v2: Rapid adapter trimming, identification, and read merging. *BMC Res. Notes* **9**, 88 (2016). doi: 10.1186/s13104-016-1900-2; pmid: 26868221
69. H. Li, R. Durbin, Fast and accurate short read alignment with Burrows-Wheeler transform. *Bioinformatics* **25**, 1754–1760 (2009). doi: 10.1093/bioinformatics/btp324; pmid: 19451168
70. H. Jónsson, A. Ginolhac, M. Schubert, P. L. F. Johnson, L. Orlando, mapDamage2.0: Fast approximate Bayesian estimates of ancient DNA damage parameters. *Bioinformatics* **29**, 1682–1684 (2013). doi: 10.1093/bioinformatics/btt193; pmid: 23613487
71. A. Prjibelski, D. Antipov, D. Meleshko, A. Lapidus, A. Korobeynikov, Using SPAdes De Novo Assembler. *Curr. Protoc. Bioinformatics* **70**, e102 (2020). doi: 10.1002/cpbi.102; pmid: 32559359
72. H. Li, Minimap2: Pairwise alignment for nucleotide sequences. *Bioinformatics* **34**, 3094–3100 (2018). doi: 10.1093/bioinformatics/bty191; pmid: 29750242
73. F. Sievers, D. G. Higgins, The Clustal Omega Multiple Alignment Package. *Methods Mol. Biol.* **2231**, 3–16 (2021). doi: 10.1007/978-1-0716-1036-7_1; pmid: 33289883
74. P. Danecek *et al*., Twelve years of SAMtools and BCFtools. *Gigascience* **10**, giab008 (2021). doi: 10.1093/gigascience/giab008; pmid: 33590861
75. B. Q. Minh *et al*., IQ-TREE 2: New models and efficient methods for phylogenetic inference in the genomic era. *Mol. Biol. Evol.* **37**, 1530–1534 (2020). doi: 10.1093/molbev/msaa015; pmid: 32011700
76. S. Kalyaanamoorthy, B. Q. Minh, T. K. F. Wong, A. von Haeseler, L. S. Jermiin, ModelFinder: Fast model selection for accurate phylogenetic estimates. *Nat. Methods* **14**, 587–589 (2017). doi: 10.1038/nmeth.4285; pmid: 28481363
77. D. T. Hoang, O. Chernomor, A. von Haeseler, B. Q. Minh, L. S. Vinh, UFBoot2: Improving the ultrafast bootstrap approximation. *Mol. Biol. Evol.* **35**, 518–522 (2018). doi: 10.1093/molbev/msx281; pmid: 29077904
78. X. Didelot, D. J. Wilson, ClonalFrameML: Efficient inference of recombination in whole bacterial genomes. *PLOS Comput. Biol.* **11**, e1004041 (2015). doi: 10.1371/journal.pcbi.1004041; pmid: 25675341
79. A. J. Drummond, R. R. Bouckaert, *Bayesian Evolutionary Analysis with BEAST* (Cambridge Univ. Press, 2015).
80. E. P. McCann *et al*., The genotype-phenotype landscape of familial amyotrophic lateral sclerosis in Australia. *Clin. Genet.* **92**, 259–266 (2017). doi: 10.1111/cge.12973; pmid: 28105640
81. A. J. Drummond, A. Rambaut, B. Shapiro, O. G. Pybus, Bayesian coalescent inference of past population dynamics from molecular sequences. *Mol. Biol. Evol.* **22**, 1185–1192 (2005). doi: 10.1093/molbev/msi103; pmid: 15703244
82. W. H. Eschenfeldt, S. Lucy, C. S. Millard, A. Joachimiak, I. D. Mark, A family of LIC vectors for high-throughput cloning and purification of proteins. *Methods Mol. Biol.* **498**, 105–115 (2009). doi: 10.1007/978-1-59745-196-3_7; pmid: 18988021
83. D. Nathans, H. O. Smith, Restriction endonucleases in the analysis and restructuring of dna molecules. *Annu. Rev. Biochem.* **44**, 273–293 (1975). doi: 10.1146/annurev.bi.44.070175.001421; pmid: 166604
84. B. A. Adler *et al*., The genetic basis of phage susceptibility, cross-resistance and host-range in *Salmonella*. *Microbiology (Reading)* **167**, ••• (2021). doi: 10.1099/mic.0.001126; pmid: 34910616
85. M. I. Love, W. Huber, S. Anders, Moderated estimation of fold change and dispersion for RNA-seq data with DESeq2. *Genome Biol.* **15**, 550 (2014). doi: 10.1186/s13059-014-0550-8; pmid: 25516281
86. O. Westphal, Bacterial lipopolysaccharides: Extraction with phenol-water and further applications of the procedure. *Methods Carbohydr. Chem.* **5**, 83 (1965).
87. J. H. Krauss, J. Weckesser, H. Mayer, Electrophoretic analysis of lipopolysaccharides of purple nonsulfur bacteria. *Int. J. Syst. Bacteriol.* **38**, 157–163 (1988). doi: 10.1099/00207713-38-2-157
88. W. S. York, A. G. Darvill, M. McNeil, T. T. Stevenson, P. Albersheim, "Isolation and characterization of plant cell

walls and cell wall components" in *Methods in Enzymology* (Academic, 1986), vol. 118, pp. 3–40.
89. T. Backman, A domesticated phage suppresses competitors in historical and modern metapopulations of pathogenic bacteria, Dryad (2024); https://doi.org/10.5061/dryad.hx3ffbgn9.
90. S. M. Latorre, Pseudomonas_tailocin, Zenodo (2024); https://doi.org/10.5281/zenodo.10794071.
91. T. Backman, Ps1524_tailocin, Zenodo (2024); https://doi.org/10.5281/zenodo.10729592.
92. A. J. Aylward, S. Petrus, A. Mamerto, N. T. Hartwick, T. P. Michael, PanKmer: K-mer-based and reference-free pangenome analysis. *Bioinformatics* **39**, btad621 (2023). doi: 10.1093/bioinformatics/btad621; pmid: 37846049

## ACKNOWLEDGMENTS

We thank S. Kamoun, P. Lang, G. Ofir, D. Petrov, and D. Weigel for comments that improved this manuscript and C. Krause, A. Rosenbauer, and M, Thiv from the Stuttgart State Museum of Natural History and O. Bossdorf from the Herbarium Tubingense for their introduction to and help in the herbaria and kind permission to sample specimens. **Funding:** This study was supported by startup funds from the University of Utah and by the National Institutes of Health (NIH grant R35 GM150722-01 to T.L.K.), The Leverhulme Trust (Philip Leverhulme Prize to H.A.B.), the Royal Society (grant RSWF\R1\191011 to H.A.B.), the UK Biological Sciences Research Council (BBSRC equipment grant BB/R01356X/1 to University College London), and the Max Planck Society (funding to the Department of Molecular Biology of the Max Planck Institute for Biology led by D. Weigel). T.B. was supported by the NIH Training Program in Microbial Pathogenesis (grant T32 AI055434). Proteomics mass spectrometry analysis was performed at the Mass Spectrometry and Proteomics Core Facility at the University of Utah. Transmission electron microscopy was performed at the Electron Microscopy Core Laboratory at the University of Utah. Mass spectrometry instrumentation was obtained through the University of Utah Research Instrumentation Fund. This work was supported in part by the US Department of Energy, Office of Science, Basic Energy Sciences, Chemical Sciences, Geosciences and Biosciences Division at DOE Center for Plant and Microbial Complex Carbohydrates at the CCRC (award DE-SC0015662 to P.A.) and by NIH National Glycoscience Resource-CCRC Service and Training (grant R24GM137782 to P.A.). A.D.G. was supported by the Dropkin Foundation and the University of Chicago Hutchinson fund. **Author contributions:** Biological discovery and conceptualization: T.B., H.A.B., T.L.K.; Computation: T.B., S.L.; Experiments: T.B., D.M.B., E.S., A.M.M., S.S., L.E., P.I.M.-K., A.M., E.B., A.H.; Methodology: T.B., S.L., A.M.D., P.A., A.D.G., J.B., H.A.B., T.L.K.; Writing: T.B., S.L., J.B., T.L.K., H.A.B. **Competing interests:** The authors declare no competing interests. **Data and materials availability:** All data and code are available in the supplementary materials and have been deposited in the following repositories. Data have been deposited to Zenodo (*67*) and Dryad (*89*). Code has been deposited to GitHub (*90*, *91*).  This research was funded in whole or in part by UK Biological Sciences Research Council (BBSRC equipment grant BB/R01356X/1), a cOAlition S organization. The author will make the Author Accepted Manuscript (AAM) version available under a CC BY public copyright license.

## SUPPLEMENTARY MATERIALS

science.org/doi/10.1126/science.ado0713
Figs. S1 to S12
Tables S1 to S5
MDAR Reproducibility Checklist

Submitted 16 January 2024; accepted 24 April 2024
10.1126/science.ado0713

# Erratum

*Post date 10 April 2025*

**Erratum for the Research Article "A phage tail–like bacteriocin suppresses competitors in metapopulations of pathogenic bacteria" by T. Backman *et al*.**

In the Research Article, "A phage tail–like bacteriocin suppresses competitors in metapopulations of pathogenic bacteria," by T. Backman *et al*. (14 June 2024, p. eado0713), the color key for Fig. 4B was inadvertently reversed. Light gray should have indicated "present" (not "absent"), and dark gray should have indicated "absent" (not "present"). The key has now been corrected.



10.1126/science.adx9434